

AN EXPERIMENTAL STUDY OF INTERCEPTION NOISE IN ELECTRON  
BEAMS AT MICROWAVE FREQUENCIES

by

Bruce A. McIntosh

A thesis submitted to the Faculty of Graduate  
Studies and Research of McGill University, in  
partial fulfilment of the requirements for the  
degree of Doctor of Philosophy

Eaton Electronics Research Laboratory  
McGill University

September, 1958

## TABLE OF CONTENTS

	<u>Page</u>
ABSTRACT .....	(i)
ACKNOWLEDGEMENTS .....	(ii)
1. INTRODUCTION .....	1
2. THEORY .....	6
I Theory of Interception Noise at Low Frequencies .....	7
II Interception Noise at High Frequencies.....	10
III Space-Charge Waves in a Drifting Electron Stream .....	25
3. APPARATUS .....	27
4. MEASUREMENTS .....	34
I Calibration of the Measuring System .....	34
II Precision and Accuracy of Measurements .....	36
III Space-Charge Wave Measurements .....	38
5. EXPERIMENTAL RESULTS AND THEIR INTERPRETATION .....	41
I Interception Noise as a Function of Magnetic Field Strength .....	41
II The Variation of Interception Noise with Gun Voltage	44
III Space-Charge Waves on an Intercepted Beam .....	45
6. CONCLUSIONS .....	55
APPENDIX 1 .....	58
APPENDIX 2 .....	63
APPENDIX 3 .....	69
APPENDIX 4 .....	75
REFERENCES .....	77

ABSTRACT

The noise added to an electron stream by the interception of a fraction of the current has been studied experimentally at a frequency of 3 kmc/s. The electron beam was produced in a demountable vacuum system by a parallel-flow Pierce gun in a confining magnetic field. A series of circular apertures and mesh grids on a plate capable of being moved within the vacuum chamber allowed the interception of various fractions of the total beam current. The excess noise caused by interception was measured at the anode of the electron gun and at various points in a drift region.

Interception noise caused by mesh grids was found to be of much greater magnitude than that caused by circular apertures. The absolute level of the excess noise and its variation with the strength of the confining magnetic field were found to be in reasonable agreement with existing theory as modified by the author.

It was shown that current interception excites a standing wave of noise along the electron beam in the drift region. Measurements made on a temperature-limited electron beam have shown that interception noise can arise in a region where noise smoothing is a consequence of processes external to the electron gun.

ACKNOWLEDGEMENTS

The author wishes to thank Professor G. A. Woonton for his supervision and encouragement during the research project. Thanks are due to Dr. E. V. Kornelsen and to Mr. R. A. McFarlane for their assistance in the design of electron guns and portions of the electronic apparatus.

The design of much of the mechanical apparatus was the outcome of many discussions with Mr. V. Avarlaid, supervisor of the Machine Shop. The care and precision with which the mechanical apparatus was constructed contributed greatly to the success of the project.

This research formed part of the work on the physics of electron beams, which is financed at the Eaton Electronics Research Laboratory by the Defence Research Board of Canada. The author is indebted to the National Research Council of Canada for granting him leave of absence in order to carry out this work, and for financial assistance in the form of three Studentships.

## CHAPTER 1

### INTRODUCTION

In modern radio communication, intelligence is frequently received in the form of small currents or voltages which must be amplified to be of further use. These signals must compete with random fluctuations of current and voltage, called "noise", which are inherent in electron tubes. In order that devices may be designed which have the maximum ability to discriminate between small signals and noise, a fundamental knowledge of noise behaviour is necessary.

The effect of noise in electronic devices operating in the portion of the frequency spectrum up to a few tens of megacycles per second has been the subject of experimental and theoretical investigations since 1918; an excellent summary is given by MacDonald (1948). With the impetus provided by the war-time development of radar, amplifier tubes for use in the thousand megacycle (or microwave) region have become of increasing interest. A large number of theoretical and experimental investigations in the past few years has been devoted to explaining the noise behaviour of such devices. Among them has been the contribution of the noise group in the Eaton Electronics Laboratory. (Kornelson 1957, Vessot 1957, Shkarofsky 1957, McFarlane 1958b).

As a part of the work of this group, the author has carried out an experimental study of interception noise, which may be defined as the excess noise created when a fraction of the current in an electron stream is intercepted by an electrode. Under certain conditions of operation of a vacuum tube, the noise in the electron stream may be less than a

maximum value known as "full shot noise". This noise reduction, called "smoothing", implies that the motions of the electrons must be to some extent correlated. The interception of a portion of the electron stream partially destroys the correlation and causes the noise in the remaining portion of the electron stream to be increased.

Although, in principle, interception noise may be avoided by eliminating interception, in practice a structure which intercepts current may be of primary importance to the operation of the tube. While it is not a fundamental phenomenon in the same sense as noise due to random thermionic emission, interception noise is nevertheless unavoidable in many types of electron tubes.

Measurements of interception noise at high frequencies have been reported in the literature (Cutler and Quate 1950, Rowe 1952, Fried and Smullen 1954) but these have been few in number and frequently only qualitative in nature.

This thesis reports an experimental investigation of interception noise at microwave frequencies. Measurements have been made of the excess noise caused by interception of various amounts of current from a long cylindrical electron beam confined by a magnetic field. Several intercepting electrodes in the form of circular apertures and mesh grids were used.

North (1940) developed a theory of interception noise which has been used successfully at low frequencies to predict the increased noisiness of multigrid tubes over the single-grid triode. This theory was believed to be inapplicable to microwave tubes for two reasons: it was based on a particular mechanism of noise smoothing which was believed to be invalid

at high frequencies; it assumed that current is intercepted by a fine mesh grid, whereas in many types of microwave tubes, current is intercepted by circular apertures.

For the purpose of analysing noise behaviour, a microwave tube utilizing a long electron beam may be divided into two regions: the electron gun, and the drift space. In the electron gun, electrons are emitted from a hot cathode and accelerated by an electric field towards the anode. The electron beam passes through a hole in the anode and enters a field-free region where it drifts at constant velocity. Noise smoothing may exist in both regions. In the electron gun it exists only when the current is limited by space charge. In the drift region, the noise varies periodically with distance along the beam somewhat analogously to standing waves on a transmission line. There is noise smoothing at the minima of the standing wave even though there may be no smoothing in the electron gun itself.

The measurements made by the author have shown that interception by a mesh grid causes much more noise than interception of the same fraction of current by a circular aperture. Fifty percent interception by a circular aperture at the anode of the electron gun produced a decrease of only 0.5 db in approximately 10 db of smoothing. Interception of an equivalent fraction of current by a mesh grid caused decreases in smoothing of up to 7 db. It is shown that North's theory is applicable at microwave frequencies provided the intercepting electrode is a grid of sufficiently fine mesh. A criterion for the required fineness of mesh has been established.

From an investigation of the effect of interception on the noise standing wave in the drift region, it was established that interception noise

is independent of the mechanism of smoothing proposed by North.

Measurements made in the drift region showed also that current interception sets up a noise standing wave which is independent of the standing wave due to noise of thermal origin. The phase relation between the two waves is of importance in the design of low-noise microwave tubes. It is believed that these measurements are the first to verify this phenomenon.

Shortly after the research reported in this thesis was begun, a significant contribution to the theory of interception noise was made by Beam (1955). He calculated the excess noise caused by interception of an electron beam by a circular aperture for the case of a beam collimated by an axial magnetic field. Since most microwave tubes require a magnetic field to confine the long electron beams used, such a theory has considerable practical importance. Beam presented experimental measurements to verify the functional variation of interception noise with magnetic field strength, but made no attempt to verify predictions concerning the magnitude of the excess noise.

It is shown in this thesis that if Beam's theory is interpreted in a slightly different manner, it predicts values of interception noise for both apertures and grids that are in agreement with experimental measurements made by the author. In two cases where the experimental conditions closely approximated the assumptions of the theory, the agreement was  $\pm 1$  db for a 5 to 1 variation in magnetic field strength. Larger discrepancies in other cases were attributed to perturbations in the electron flow, in particular to the variation of direct current density with radius in the beam. For circular apertures intercepting current near the beam edge, better agreement with experiment has been obtained by modifying the

the theory to take into account non-uniform current density. The actual variation of current density with radius was found to deviate widely from the theoretical form.

## CHAPTER 2

### THEORY

There are two basic methods of dealing with electron beam noise problems. When the statistics of a fluctuation process are known, the mean square of the fluctuation quantity can be calculated directly. The classic examples of this method are: the mean square noise current at the anode of a diode whose emission is temperature limited, which was calculated by Schottky (1918); and the mean square velocity fluctuation in the region immediately in front of the cathode which was calculated by Rack (1938). In other cases, the manner in which the statistics of the fluctuation process are modified by electromagnetic fields and the geometry of electron flow is not known. This leads to what may be called the "signal propagation" method. Theories of the propagation of sinusoidal signals in electron streams are fairly well established. For any portion of an electron beam to which these theories are applicable it may be assumed that "output" power as a function of "input" power is known. If the input is chosen at a point where the mean square noise fluctuation is known, this may be taken as proportional to the average value of the input power at the signal frequency. Hence the noise power at the output can be calculated.

This chapter is concerned primarily with the first method which is of use in calculating interception noise at the point where current interception occurs. For low frequency tubes, such a calculation gives directly the increased noise in the anode current. In microwaves tubes, in contrast, the signal theories must be employed to determine the behaviour of interception noise beyond the point of interception.

I THEORY OF INTERCEPTION NOISE AT LOW FREQUENCIES

The low frequency theories of noise smoothing and of interception noise as exemplified by that of North (1940) make use of a semi-statistical approach. North's theory is based primarily on the mechanism of control of anode current by electron space charge as calculated by Fry (1921) and Langmuir (1923).

Electrons are emitted from a hot cathode in random numbers in any given time interval, and with random velocities. If the cathode temperature is low and the anode voltage high, all emitted electrons are accelerated towards the anode and the noise in the anode current is given by the familiar shot-noise relation

$$\overline{i_n^2} = 2eI_0 \Delta f. \quad (2-1)$$

The quantity  $\overline{i_n^2}$  may be defined as the average noise power dissipated in a resistance of one ohm in a bandwidth  $\Delta f$ .  $I_0$  is the direct anode current and  $e$  is the magnitude of the electron charge.

When the temperature of the cathode is increased, a state is reached, for a given anode voltage, where not all of the emitted electrons are drawn off to the anode. The space charge immediately in front of the cathode gives rise to a negative potential region. Electrons leaving the cathode are subjected to a retarding field and only those which have sufficient initial velocity are able to surmount the potential barrier and reach the anode. The value of the potential minimum determines the anode current in such a manner that it is relatively insensitive to changes in cathode temperature and hence to fluctuations in the total emission current. If a sudden increase in emission current occurs, the potential minimum deepens

and allows a smaller fraction of the total emission current to reach the anode. The potential minimum is said to produce a compensating pulse of current of opposite sign to the initial fluctuation. If the process were perfect, fluctuations in the emission current that give rise to full shot noise in the temperature-limited case, would not be transferred into anode current fluctuations, and consequently the anode current would be noiseless. The actual degree of noise reduction is usually expressed in the form

$$\overline{i_n^2} = \Gamma^2 2e I_0 \Delta f \quad (2-2)$$

where  $\Gamma^2$  is a smoothing factor ( $\Gamma^2 < 1$ ) calculated on the basis of the Fry-Langmuir diode theory.

A fluctuation in emission from a small element of area on the cathode surface will produce a shift in the potential minimum and a corresponding compensating fluctuation in the anode current. Although the initial fluctuation is localized to a small area, the compensating fluctuation is postulated by North to be spread out over a much larger area of the electron stream. Hence, if the current stream divides between two electrodes, it may be that the initial fluctuation all arrives at electrode #1 say, while the compensating fluctuation divides between the two electrodes. Consequently, the fluctuation in the current of electrode #1 is not fully reduced and electrode #2 has received an added fluctuation. The noise in each electrode is thereby increased.

In order to avoid any question of the actual spatial extent of the compensating fluctuation, North assumes that interception takes place at a very fine mesh grid. He may then assume that the compensating current always divides between the electrodes in proportion to their d-c currents.

A Simplified derivation of North's result has been given by Robinson and Kompfner (1951). They consider interception of a fraction  $\alpha$  of the total d-c current  $I_{01}$ . (The subscript  $_1$  will be used to denote quantities before interception and  $_2$  after interception.) The noise in the remaining  $1-\alpha$  of the current is,

$$\overline{i_{2n}^2} = \left[ \Gamma_1^2 + \alpha (1 - \Gamma_1^2) \right]^2 (1 - \alpha) 2e I_{01} \Delta f \quad (2-3)$$

Since

$$I_{02} = (1 - \alpha) I_{01}$$

the effective smoothing factor after interception is

$$\Gamma_2^2 = \frac{\overline{i_{2n}^2}}{2e I_{02} \Delta f} = \Gamma_1^2 + \alpha (1 - \Gamma_1^2) \quad (2-4)$$

North (1940c) verified this expression experimentally at low frequencies for certain types of tube structures. These were such that the idealized assumptions of the theory were approximately fulfilled. In spite of this success, the "model" that North proposed to explain interception noise is difficult to accept. For example, it is difficult to visualize an intercepting mesh grid which always divides the compensating fluctuation but never the initial fluctuation. Electrons are emitted with a Maxwellian distribution of velocities in the transverse direction so that emission from a small element of cathode area is spread over a considerably larger area before it has travelled very far. Further, at microwave frequencies transit times become long compared with the period of the frequency so that the concept of compensating fluctuations completely correlated (in time) with the initial fluctuations becomes questionable. There is reasonable

agreement between high frequency theories based on complete neglect of the mechanism of smoothing proposed by North and experimental measurements (Cutler and Quate 1950).

## II INTERCEPTION NOISE AT HIGH FREQUENCIES

Robinson (1954) argued that interception noise would arise whatever the mechanism of smoothing and that results of North's theory would be applicable even at microwave frequencies. Beam (1955) demonstrated that the theory of interception noise could be based on the random probability of interception of electrons by the intercepting grid. It should be noted that this concept is not new (Schottky 1938; Lawson and Uhlenbeck 1950), but the author feels that it has not received sufficient emphasis and that too literal an interpretation of North's concept of compensating fluctuations has led to many misconceptions in the theory of interception noise.

The following theory follows the presentation given by Beam.

It is assumed that the intercepting electrode is a fine mesh grid so that the probability of interception is uniform over the entire cross section of the electron stream. The total d-c current before interception is  $I_{o1}$ . After interception it is

$$I_{o2} = k_o I_{o1}$$

That is,  $k_o$  is the transmission factor of the grid. For small intervals of time, random fluctuations in the fraction of current transmitted will be observed. Thus the transmission factor measured in a small interval of time  $\Delta t$  may be written as

$$k_o + k_1$$

where the  $k_1$  are random fluctuations such that

$$\bar{k}_1 = 0$$

The bar is used to denote either a time average or an ensemble average. The latter implies the average of the given quantity for a large number of identical systems as opposed to the average over a long period of time of observation on a single system. For all cases dealt with in noise theory, the two methods of averaging yield the same result. Ensemble averages frequently are more easily determined since they are well known from the mathematical theory of probability for certain types of statistical distributions.

The number of electrons approaching the plane of interception in the time interval  $\Delta t$  also exhibits fluctuations. This number may be expressed as an average value  $\bar{n}$  plus a fluctuation  $\Delta$  where  $\bar{\Delta} = 0$ .

The incident electrons cannot be characterised by a single velocity but rather by a distribution of velocities. If the velocity distribution is divided into a finite number of velocity classes, the average number of electrons in each velocity class will be different. By summing over all velocity classes, the total number of electrons transmitted through the intercepting grid in a time interval  $\Delta t$  is

$$\sum_s (\bar{n}_s + \Delta_s) (k_0 + k_{1s})$$

The current transmitted is therefore

$$I_2 = \frac{e}{\Delta t} \sum_s (\bar{n}_s + \Delta_s) (k_0 + k_{1s}) \quad (2-5)$$

The d-c component, which is

$$\frac{e}{\Delta t} k_o \sum_s \bar{n}_s = k_o I_{o1} = I_{o2} \quad , \quad (2-6)$$

may be subtracted to leave the fluctuation

$$i_2 = \frac{e}{\Delta t} \sum_s (k_o \Delta_s + \bar{n}_s k_{1s} + \Delta_s k_{1s}) \quad .$$

The ensemble average is

$$\overline{i_2^2} = \left(\frac{e}{\Delta t}\right)^2 \overline{\sum_{r,s} (k_o \Delta_r + \bar{n}_r k_{1r} + \Delta_r k_{1r}) (k_o \Delta_s + \bar{n}_s k_{1s} + \Delta_s k_{1s})} \quad .$$

It is assumed that the emission fluctuations and interception fluctuations are statistically independent. That is,

$$\overline{\Delta_r k_{1s}} \equiv 0, \quad \text{all } r \text{ and } s \quad .$$

Also, the interception fluctuations in one velocity class are independent of those in all other velocity classes.

$$\overline{k_{1r} k_{1s}} = 0, \quad r \neq s \quad .$$

This condition is not true of the current fluctuations if smoothing exists. Then,

$$\overline{i_2^2} = \left(\frac{e}{\Delta t}\right)^2 \left[ k_o^2 \sum_{r,s} \overline{\Delta_s \Delta_r} + \sum_s \overline{(\bar{n}_s k_{1s})^2} + \sum_s \overline{k_{1s}^2 \Delta_s^2} \right] \quad (2-7)$$

The third term in the brackets is a second order fluctuation which Beam has shown to be negligible. The second term is the ensemble average of the square of the deviation from the average transmission  $k_o \bar{n}_s$ . These numbers have a Bernouli distribution (Goldman 1948), hence

$$\overline{(\bar{n}_s k_{1s})^2} = k_o \bar{n}_s (1 - k_o) \quad .$$

The first term involves the initial fluctuations modified by  $k_o^2$ .

At this point a distinction between the ensemble average of a current fluctuation and mean square noise current must be made. The ensemble average is carried out in the time domain whereas the mean-square noise current involves the power spectrum in the frequency domain. If the noise is denoted by  $\overline{i_{2n}^2}$ , then Beam has shown that

$$\overline{i_{2n}^2} = 2 \Delta t \Delta f \overline{i_2^2} ,$$

where  $\overline{i_2^2}$  is the ensemble average for the time interval  $\Delta t$  as given in Equation (2-7).

The noise in the current stream before interception may be written as

$$\overline{i_{1n}^2} = \Gamma_1^2 2e I_{o1} \Delta f$$

Then

$$\overline{i_{2n}^2} = k_o^2 \Gamma_1^2 2e I_{o1} \Delta f + k_o(1 - k_o) 2e I_{o1} \Delta f \quad (2-8)$$

Equation (2-8) may be rearranged to yield

$$\overline{i_{2n}^2} = k_o \Gamma_1^2 2e I_{o1} \Delta f + (1 - \Gamma_1^2) k_o (1 - k_o) 2e I_{o1} \Delta f \quad (2-9)$$

which is identical with Equation (2-3) if it is noted that  $1 - k_o = \alpha$ .

Beam identifies the first term of Equation (2-8) with the original noise in the beam, and the second term as the excess noise added by interception. That this is incorrect may be seen intuitively from the following argument.

If the incident beam is unsmoothed, i.e.  $\Gamma_1^2 = 1$ , then provided the interception is uniform over the cross section, Equations (2-8) and (2-9)

yield the same result, namely that the noise after interception is full shot noise in the current  $I_{c2}$ .

$$\overline{i_{2n}^2} = k_0 2e I_{o1} \Delta f = 2e I_{o2} \Delta f, \Gamma_1^2 = 1.$$

Later in his paper, Beam treats the case of interception by a circular aperture and shows that the noise is

$$\overline{i_{2n}^2} = \Omega_1^2 \Gamma_1^2 2e I_{o1} \Delta f + \Omega_2 2e I_{o1} \Delta f$$

(The notation  $\Omega_1$ , and  $\Omega_2$  is used to conform to that of Beam. The subscripts do not indicate values before and after interception).  $\Omega_1$  is essentially equal to the transmission factor of the aperture. That is,

$$\Omega_1 = k_0$$

The factor  $\Omega_2$  replaces  $k_0 (1 - k_0)$  and in many cases,

$$\Omega_2 \ll k_0 (1 - k_0)$$

In fact it is possible for  $\Omega_2$  to approach zero. Then if the incident beam is unsmoothed, the noise in the intercepted beam is

$$\begin{aligned} \overline{i_{2n}^2} &\approx \Omega_1^2 2e I_{o1} \Delta f \\ &\approx k_0 2e I_{o2} \Delta f \end{aligned}$$

which implies that the shot noise in the transmitted beam is reduced by the transmission factor. Experimental evidence is to the contrary. Although the separation of terms in Equation (2-9) is artificial, it appears to be the more logical form, and is supported by the experimental measurements made by the author.

A CRITERION FOR UNIFORM PROBABILITY OF INTERCEPTION

The validity of the assumption that the probability of interception is the same at all points on a cross section of the electron stream may be examined qualitatively for a particular geometrical shape of intercepting electrode by considering the mechanism which gives rise to random interception.

If electrons follow straight line trajectories perpendicular to the cathode, random interception, and hence interception noise, cannot occur. Imperfections in the electrostatic focussing fields in the electron gun may give rise to curved trajectories and hence to the possibility of random interception, since the electrons start with random initial velocities. This effect would be correlated with the longitudinal velocity fluctuations, and would be difficult to calculate. Random interception which is statistically independent of longitudinal fluctuations must arise from the random transverse velocities with which electrons are emitted. The trans-  
velocity distribution is

$$\frac{dN_{v_T}}{N} = \frac{m}{kT_c} \exp \left[ - \frac{m v_T^2}{2kT_c} \right] v_T dv_T \quad (2-10)$$

- $v_T$  is the transverse velocity,
- $m$  the mass of electron,
- $k$  Boltzmann's constant,
- $T_c$  the cathode temperature.

Equation (2-10) gives the fraction of the total number of electrons  $N$  emitted per second per unit area that, on the average, would be found with transverse velocities between  $v_T$  and  $v_T + dv_T$ .

For an infinite, parallel-plane diode or a Pierce-type electron gun (Pierce 1949), the accelerating field is in the direction perpendicular to the cathode. Because of its initial transverse velocity, an electron which starts from a point  $P(r, \theta)$  on the cathode, will arrive at a point  $P_1(r_1, \theta_1)$  at a plane farther down the beam. The  $N_p$  electrons emitted per second from a small element of area at  $P$  may be considered to arrive at a plane (say the anode plane) distributed over an area with  $(r, \theta)$  as centre. If the anode potential is high, the mean spread in cathode - anode transit time due to initial velocities is negligibly small. Then at the anode, the deviation of an electron from the point  $(r, \theta)$  will be

$$\rho = \tau v_T ,$$

where  $\tau$  is the transit time and  $v_T$  the initial transverse velocity. The radial distribution of electrons about the point  $(r, \theta)$  will be of the form

$$\frac{dN_\rho}{N_p} = \frac{m}{kT_c} \exp \left[ - \frac{m \rho^2}{2k T_c \tau^2} \right] \frac{d\rho}{\tau} .$$

The mean square transverse velocity at the cathode is

$$u_T^2 = \frac{2k T_c}{m} .$$

A "mean spreading radius",  $\rho_e$ , may be defined by

$$\rho_e = \tau u_T .$$

Then

$$\frac{dN_\rho}{N_p} = \exp \left[ - \frac{\rho^2}{\rho_e^2} \right] \frac{2\pi \rho d\rho}{\pi \rho_e^2} . \quad (2-11)$$

Thus a criterion for uniform probability of interception over a mesh

grid may be set up by specifying that the effective area of one grid module shall be much less than the mean spreading area  $\pi \rho_e^2$ . If the grid openings are larger than the mean spreading area the effective area over which interception of electrons will be random, will be much smaller than the total beam area.

For a typical electron gun (an experiment gun to be described later),

$$u_T \sim 2 \times 10^5 \text{ meters/sec.}$$

$$\tau \sim 10^{-9} \text{ sec.}$$

Hence,

$$\rho_e \sim 0.2 \text{ mm.}$$

It may be noted that in a practical electron gun, perturbations in the accelerating and focussing fields may add considerably to the spreading.

#### Non-Uniform Interception

To treat the case of non-uniform interception probability, the transmission factor  $k_0$  may be considered to be a function of transverse coordinates in the electron stream. Let  $k_0(r)$  be the probability that electrons associated with a given point in the beam cross section will be transmitted through the intercepting electrode. Cylindrical symmetry is assumed. For a circular aperture of radius  $r_a$ , the probability of electrons near the centre of the beam being intercepted is negligibly small.

That is,

$$\left. \begin{aligned} k_0(r) &= 1 \\ k_0(r) [1 - k_0(r)] &= 0 \end{aligned} \right\} r \ll r_a$$

In the outer edge of the beam, well beyond the transmitting hole, the probability of an electron being transmitted is negligibly small so that

$$k_o(r) = 0 = k_o(r) [1 - k_o(r)] , \quad r \gg r_a$$

Thus the product  $k_o(r) [1 - k_o(r)]$  which appears in the interception noise Equation (2-9) will have value only over a region near the edge of the aperture and the value of this product averaged over the entire beam cross section will be much smaller than that predicted by the d-c transmission.

Beam (1955) has shown that a logical extension of the theory to the case of non-uniform interception is to replace the transmission factor  $k_o$  with corresponding averages of  $k_o(r)$  and  $k_o(r) [1 - k_o(r)]$  over the beam cross section. He defines

$$\Omega_1 = \frac{\int k_o(r) J(r) dA}{\int J(r) dA} \quad (2-12a)$$

$$\Omega_2 = \frac{\int k_o(r) [1 - k_o(r)] J(r) dA}{\int J(r) dA} \quad (2-12b)$$

$J(r)$  is the d-c current density which in general may be a function of transverse coordinates. The integrals are over the entire cross-sectional area of the incident beam.

$$\int J(r) dA = I_{o1}$$

From the definition of  $k_o(r)$ ,

$$\int k_o(r) J(r) dA = I_{o2}$$

Hence  $\Omega_1$  is the average transmission factor

$$\Omega_1 = \frac{I_{o2}}{I_{o1}} \quad (2-13)$$

The expression for the noise content of a beam after interception, as modified by the author, becomes

$$\overline{i_{2n}^2} = \Omega_1 \Gamma_1^2 2e I_{o1} \Delta f + (1 - \Gamma_1^2) \Omega_2 2e I_{o1} \Delta f \quad (2-14)$$

With the aid of Equation (2-13), this may be normalised to full shot noise in the intercepted beam.

$$\frac{\overline{i_{2n}^2}}{2e I_{o2} \Delta f} = \Gamma_2^2 = \Gamma_1^2 + (1 - \Gamma_1^2) \frac{\Omega_2}{\Omega_1} \quad (2-15)$$

#### Calculation of $\Omega_1$ and $\Omega_2$

Case 1. The particular case treated by Beam is that of a circular aperture intercepting a beam confined by an axial magnetic field.

An electron which is emitted from the cathode with transverse velocity  $v_T$  follows a spiral trajectory, the axis of the spiral being parallel to the magnetic field and the radius being

$$\rho = v_T / (B \frac{e}{m}) \quad (2-16)$$

where B is the strength of the magnetic field. For a point P (r,  $\theta$ ) on some cross section of the beam, there are  $N_p$  electrons which execute spirals with P as centre. The probability of finding a certain fraction of these electrons with radii between  $\rho$  and  $\rho + d\rho$  is the same as the probability of finding that fraction with transverse velocities between  $v_T$  and  $v_T + dv_T$ . Hence the radial probability distribution is given by

$$\frac{dN_p}{N_p} = \frac{(Be)^2}{mk T_c} \exp \left[ - \frac{(Be)^2}{2 mk T_c} \rho^2 \right] \rho d\rho \quad (2-17)$$

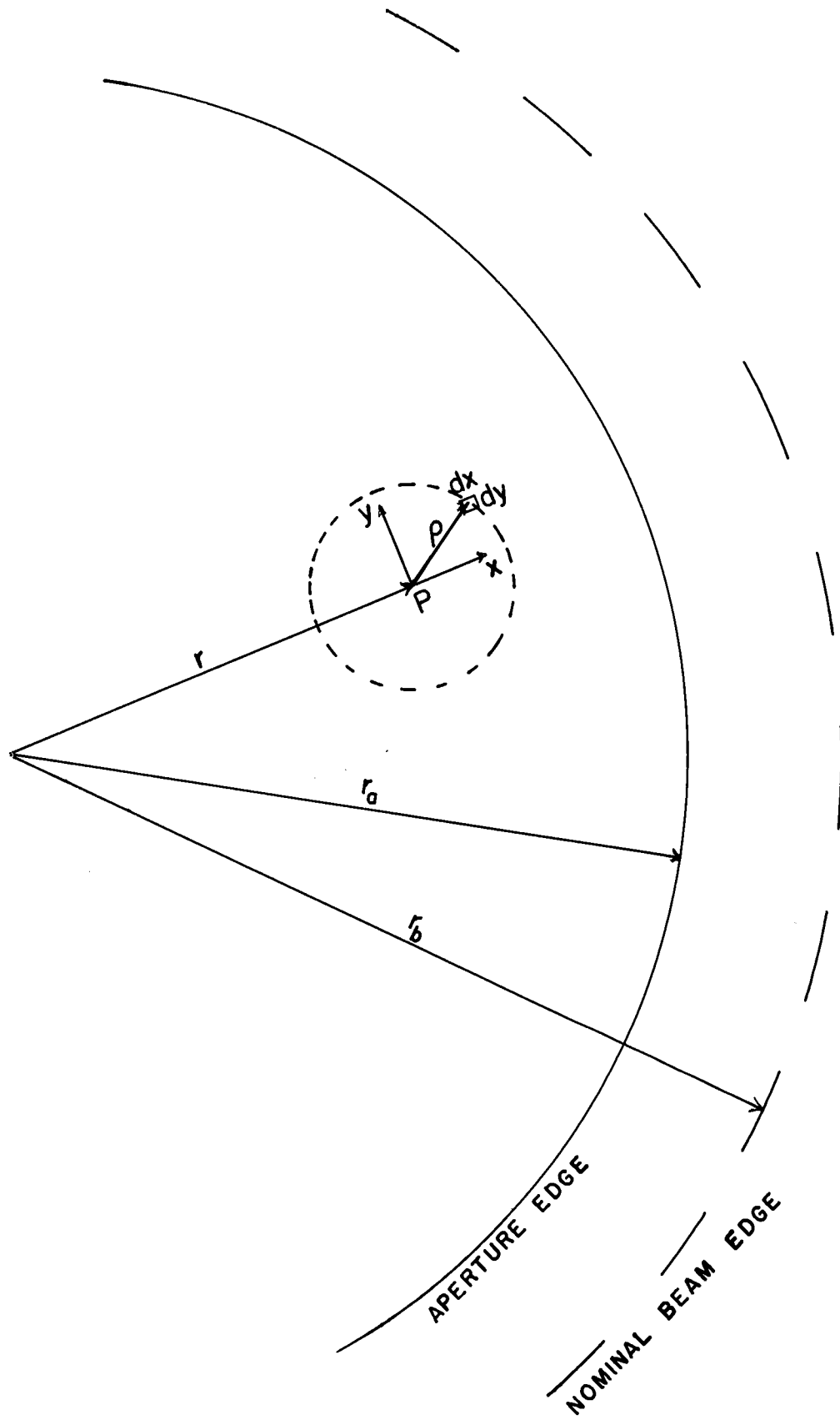


FIGURE 2-1

$$= \exp(-a^2 \rho^2) \frac{2 \rho d\rho}{1/a^2} \quad (2-18)$$

where 
$$a^2 = \frac{(Be)^2}{2 mkT_c} \quad (2-19)$$

By comparing Equation (2-18) with (2-11) it may be seen that  $\frac{1}{a}$  is equivalent to the mean spreading radius defined previously.

Because most of the  $dN_\rho$  electrons cluster within a very small radius about P, they may be considered to exist at P insofar as longitudinal interactions are concerned. Nearly two-thirds of the electrons associated with P have radii less than  $\frac{1}{a}$ . For a typical case,  $B = 500$  gauss,  $T_c = 1300^\circ\text{k}$ , and  $\frac{1}{a} = .02$  mm.

Figure 2-1 illustrates the case of a beam of nominal radius  $r_b$ , intercepted by a circular aperture of radius  $r_a$ . Of all the electrons associated with the point P at radius  $r$ , the fraction transmitted may be found by integrating the probability distribution in  $\rho$  over the aperture area. This results in a transmission factor  $k_o(r)$  given by (Beam 1955),

$$k_o(r) = \frac{1}{2} [1 + \text{erf } a(r_a - r)] \quad (2-20)$$

where the error function is defined by

$$\text{erf } y = \frac{2}{\sqrt{\pi}} \int_0^y e^{-x^2} dx$$

The functions  $k_o(r)$  and  $k_o(r) [1 - k_o(r)]$  are sketched in Figure 2-2.

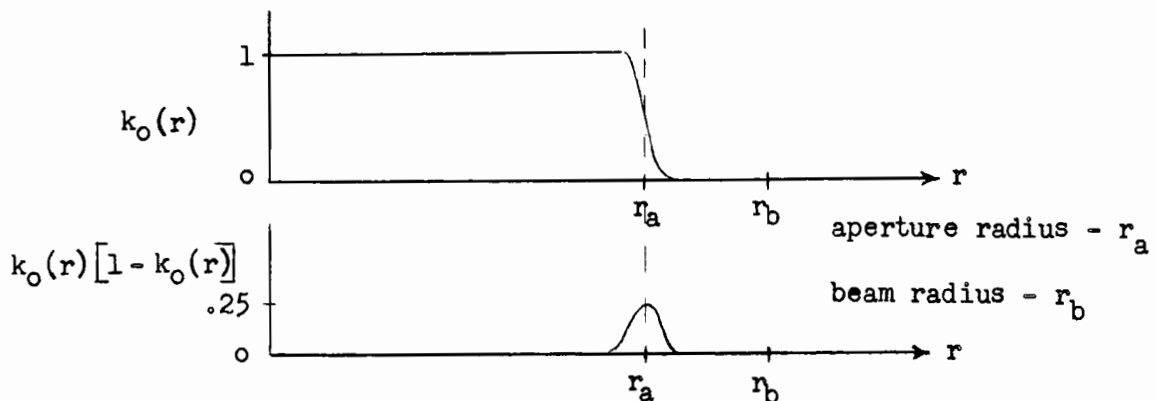


Figure 2-2

Assuming incident current density constant for  $0 \leq r \leq r_b$ , Equations (2-12) yield

$$\Omega_1 = \int_0^1 [1 + \operatorname{erf} a(r_a - ur_b)] u du \quad (2-21)$$

$$\Omega_2 = \frac{1}{2} \int_0^1 [1 - \operatorname{erf}^2 a(r_a - ur_b)] u du \quad (2-22)$$

where  $u$  is a normalised radius

$$u = \frac{r}{r_b}.$$

The evaluation of these integrals is considered in Appendix I. It is shown that for all practical purposes,

$$\Omega_1 = \left(\frac{r_a}{r_b}\right)^2, \quad r_a \leq r_b. \quad (2-23)$$

For  $r_a \geq r_b$ ,  $\Omega_1$  is approximately unity but  $1 - \Omega_1$  is of significance. This is shown in Fig. 2-3 where  $1 - \Omega_1$  is plotted versus  $r_a/r_b$  for various values of  $ar_a$ .

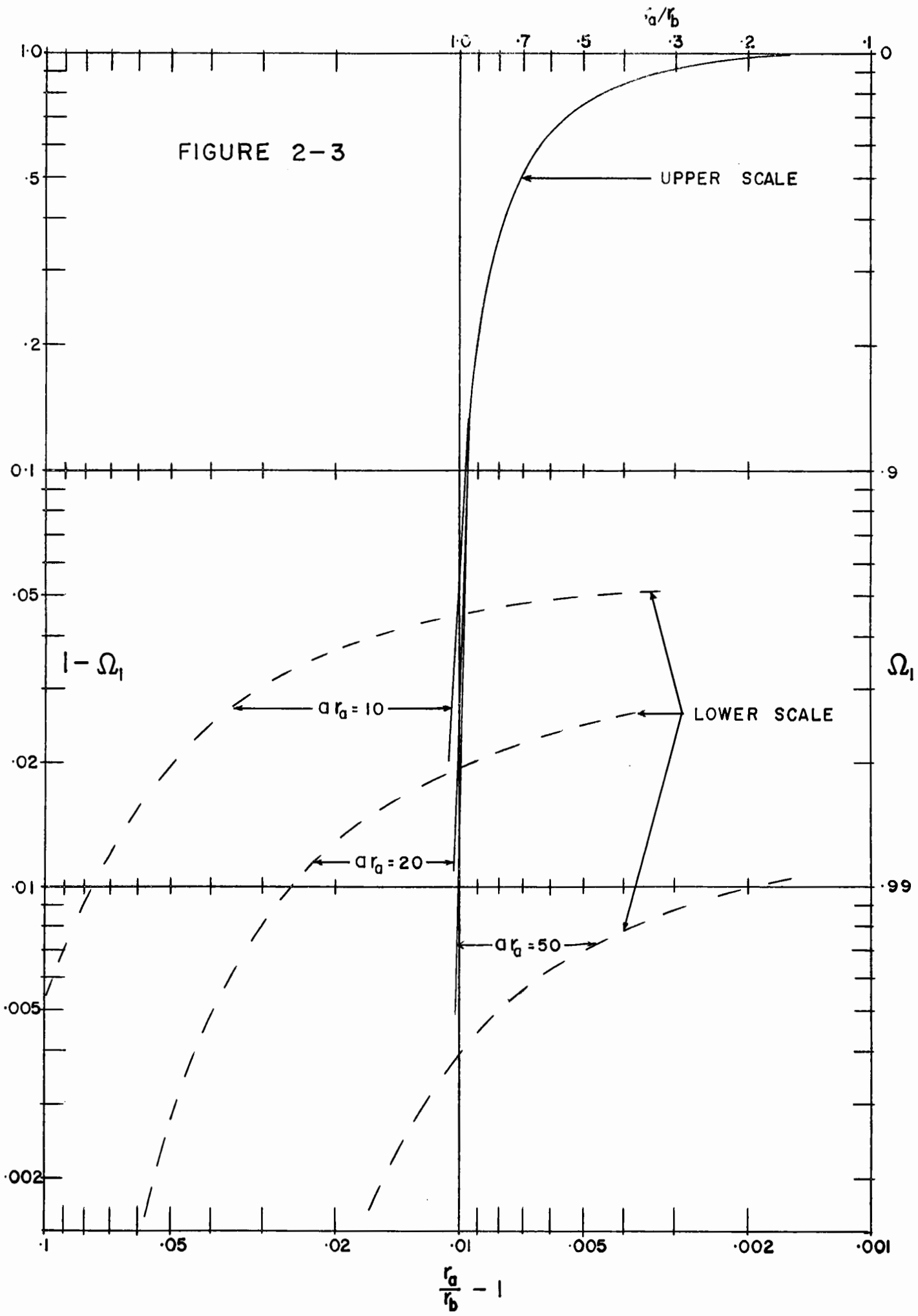
An analytic expression for  $\Omega_2$  which is valid over a wide range of magnetic field strengths is,

$$\Omega_2 = \frac{\pi}{4} \frac{r_a}{ar_b^2} \left[ \frac{1 + \operatorname{erf} \frac{2}{\sqrt{\pi}} ar_a \left(\frac{r_b}{r_a} - 1\right)}{2} \right]$$

and hence

$$\frac{\Omega_2}{\Omega_1} = \frac{\pi}{4} \frac{1}{ar_a} \left[ \frac{1 + \operatorname{erf} \frac{2}{\sqrt{\pi}} ar_a \left(\frac{r_b}{r_a} - 1\right)}{2} \right] \quad (2-24)$$

The function in brackets in Equation (2-24) has been plotted versus  $r_a/r_b$  in Fig. 2-4. It is seen to be constant if  $r_a/r_b$  is somewhat less than unity and to decrease rapidly near the beam edge. In the region where



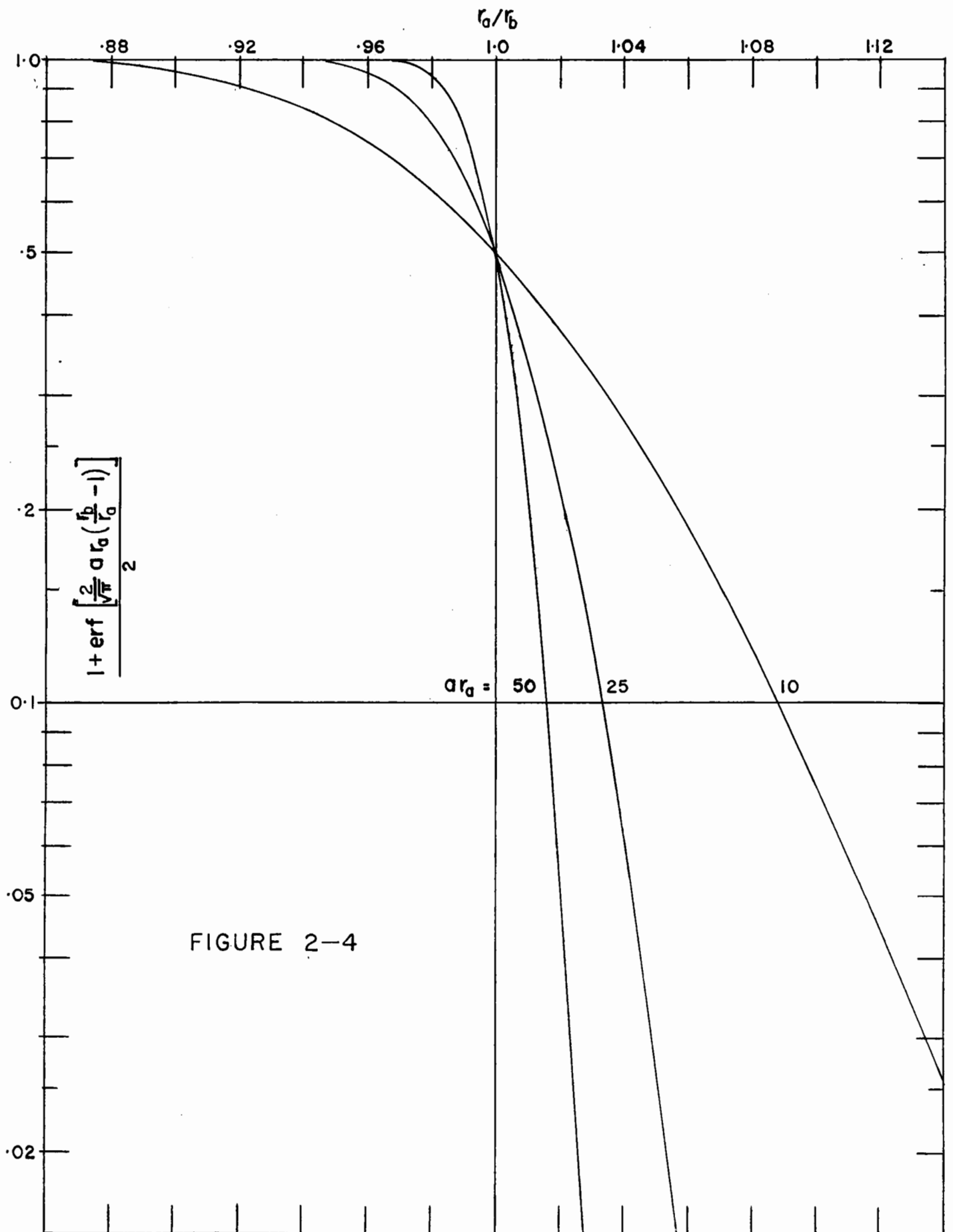


FIGURE 2-4

this function is constant, the excess noise due to interception is essentially given by

$$\frac{\Omega_2}{\Omega_1} = \frac{\pi}{4} \frac{1}{ar_a}$$

~  $\frac{\text{mean spreading radius}}{\text{radius of the intercepting aperture}}$

It is interesting to note that this expression is independent of beam radius.

Of most interest to the tube designer is the magnitude of interception noise for very small amounts of intercepted current; that is, for values of  $r_a/r_b$  nearly equal to unity. Here, Beam's theory predicts that (see Appendix 1)

$$\Omega_2 \rightarrow 1 - \Omega_1$$

ie., that interception noise approaches the North value. Beam assumes that the current density in the incident beam is constant for  $0 < r < r_b$  and is zero for  $r > r_b$ . This is unrealistic since the spiralling of electrons near the edge of the beam tends to "smear out" the edge.

It is shown in Appendix 4 that the radial dependence of current density has the same form as the transmission factor  $k_o(r)$  for  $r_a = r_b$ . That is

$$\frac{J(r)}{J_o} = [1 + \text{erf } a (r_b - r)] \quad (2-25)$$

where  $J_o$  is the average current density given by

$$J_o = \frac{I_{o1}}{\pi r_b^2}$$

Equation (2-25) has been utilized in conjunction with Equation (2-12b)

to calculate modified values of  $\Omega_2$ . The integration was carried out numerically. Representative results are listed in Table 2-I.

TABLE 2-I

Calculated values of  $\Omega_2$  modified to take into account radial variation of current density.

<u>ar<sub>a</sub></u>	<u><math>\frac{r_a - 1}{r_b}</math></u>	<u><math>\Omega_2</math> modified</u>	<u><math>\Omega_2</math> Beam</u>
50	- 0.01	$1.0 \times 10^{-2}$	$1.3 \times 10^{-2}$
	0	0.59	0.80
	0.01	0.24	0.35
20	- 0.025	2.5	2.9
	0	1.5	2.0
	0.025	0.59	0.80
10	- 0.05	5.0	6.0
	0	2.9	3.9
	0.05	1.2	1.7

Although this first order correction yields a reduction in  $\Omega_2$  of only 1 to 2 db, it does indicate that the thinning-out of current density near the beam edge tends to reduce the effect of interception.

Case 2 MESH GRIDS

Beam's theory may be extended to mesh grids in the following manner. The electron beam may be divided into a bundle of smaller beams each of which is associated with one opening in the grid. The fraction of current intercepted from one of the small beams is equal to the fraction inter-

cepted from the whole stream provided the current density is reasonably uniform over each of the small beams. A smoothing factor  $\Gamma_2^2$  may be calculated for one of the small beams in the same manner as for a single aperture, and since  $\Gamma_2^2$  is a measure of noise per unit current, the value thus calculated applies to the whole beam. This analysis neglects possible interaction among the small beams, i.e., the fact that the small beams have no "edge", and that the radii of spiralling electrons may be large enough to overlap several grid modules. Such effects should be small if the mean spreading radius  $\frac{1}{a}$  is less than the radius of one of the grid openings. When  $\frac{1}{a}$  becomes greater than this radius, the excess noise will approach the North value.

### Case 3 NO CONFINING MAGNETIC FIELD

An estimate of the excess noise produced in this case may be made by using the mean spreading radius due to transit time (as defined in Equation (2-11)) in place of  $\frac{1}{a}$  in the foregoing calculations.

### III Space-Charge Waves in a Drifting Electron Stream

When alternating current density and velocity modulation are excited in an electron stream drifting with constant velocity  $u_0$ , it is well known that their variation with distance  $z$  along the beam has the form (Hutter 1952-53),

$$J(z) = \left[ J_a \cos\left(\frac{\omega_p z}{u_0}\right) - j \frac{\omega}{\omega_p} \frac{J_0}{u_0} v_a \sin\left(\frac{\omega_p z}{u_0}\right) \right] \exp\left(-j \frac{\omega z}{u_0}\right) \quad (2-26)$$

$$v(z) = \left[ v_a \cos\left(\frac{\omega_p z}{u_0}\right) - j \frac{\omega_p}{\omega} \frac{u_0}{J_0} J_a \sin\left(\frac{\omega_p z}{u_0}\right) \right] \exp\left(-j \frac{\omega z}{u_0}\right) \quad (2-27)$$

$J_a, v_a$  are the initial values of the modulation at the plane  $z = 0$   
 $\omega = 2\pi \times$  the modulation frequency.

$\omega_p$  is the "plasma angular frequency" given by

$$\omega_p^2 = \frac{e}{m\epsilon_0} \frac{J_0}{u_0}$$

$J_0$  is the direct current density.

Time dependence  $\exp(-j\omega t)$  is understood.

The theory assumes that the modulation amplitudes  $J$  and  $v$  are small compared with the d-c values  $J_0$  and  $u_0$  respectively, and also that the beam is infinite in lateral extent.

When the beam is finite, as in a practical tube, the modulation quantities may vary with radius (Hahn 1939; Ramo 1939). For example, the current density modulation is,

$$J(z, r) = \sum_n A_n J_0(T_n r) \exp(-j \beta_n z) \quad (2-28)$$

This gives rise to an infinite number of "modes" of propagation, the radial dependence of which is given by the zero'th order Bessel functions  $J_0(T_n r)$ . The radial propagation constants  $T_n$  are determined by matching field quantities at the edge of the beam. The mode amplitudes  $A_n$  are determined by the excitation at the input plane. The longitudinal propagation constant is

$$\beta_n = \frac{\omega}{u_0} \pm p_n \frac{\omega_p}{u_0} \quad (2-29)$$

Where  $p_n$  is called the "plasma reduction factor" for the n'th mode (Watkins 1952).

Since this theory also applies to narrow-band noise, it may be seen

from Equation (2-26) that there exists a standing wave of noise power in the beam. In the infinite beam case, the standing wave has finite minima if  $J_a$  and  $v_a$  are uncorrelated noise sources. For physical beams, finite minima are predicted even in the case of single source excitation ( $v_a = 0$ , say) since the space-charge wavelength is different for each of the higher order modes.

Beam (1955) has calculated the excess velocity fluctuations caused by current interception. Thus interception is a source of current and velocity fluctuations which will excite a standing wave in a drifting electron stream. The contributions of interception noise velocity and of higher order modes to the finite minima in an interception-produced space-charge wave are investigated in more detail in Appendix 3.

CHAPTER 3

Apparatus

Figure 3-1 is a photograph of the apparatus used to make interception noise measurements. The important and central portion of the apparatus is a vacuum chamber in which an electron gun and an intercepting electrode could be moved longitudinally with respect to a resonant cavity mounted on the right end of the long brass chamber. The large solenoid, mounted on wheels and capable of being rolled over the vacuum chamber, served to collimate the electron beam. The rack-like table was used to mount electronic apparatus.

Figure 3-2 is an exploded view of the components within the vacuum chamber; the outer vacuum jacket has been removed. The electron gun and intercepting electrodes were mounted on frames which slid on teflon inserts along the inner surface of the brass tube seen at right. Over a longitudinal distance of 40 centimeters in which the motion took place, the lateral deviation of the sliding structures was less than 0.07 millimeters. Since the plungers which moved these structures had to be located off centre, the frames were made long enough to prevent binding due to flexing or twisting of the plungers. The frame carrying the intercepting electrodes consisted of two annular rings which allowed it to slide back over the cavity. The intercepting electrodes could then be positioned immediately in front of the cavity.

The intercepting electrodes used were three apertures - of diameters .080", .060", .040", - and two mesh grids. The grids were a standard type used by Varian Associates in the manufacture of klystrons. One of the

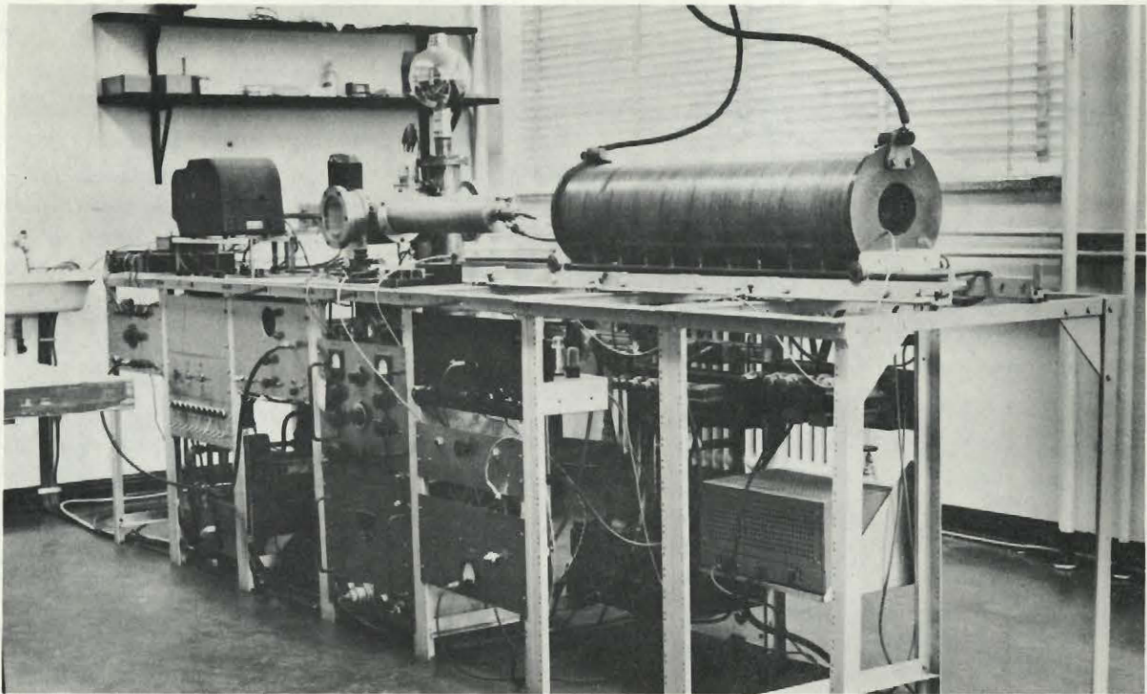


FIG. 3-1 APPARATUS USED TO MEASURE INTERCEPTION NOISE

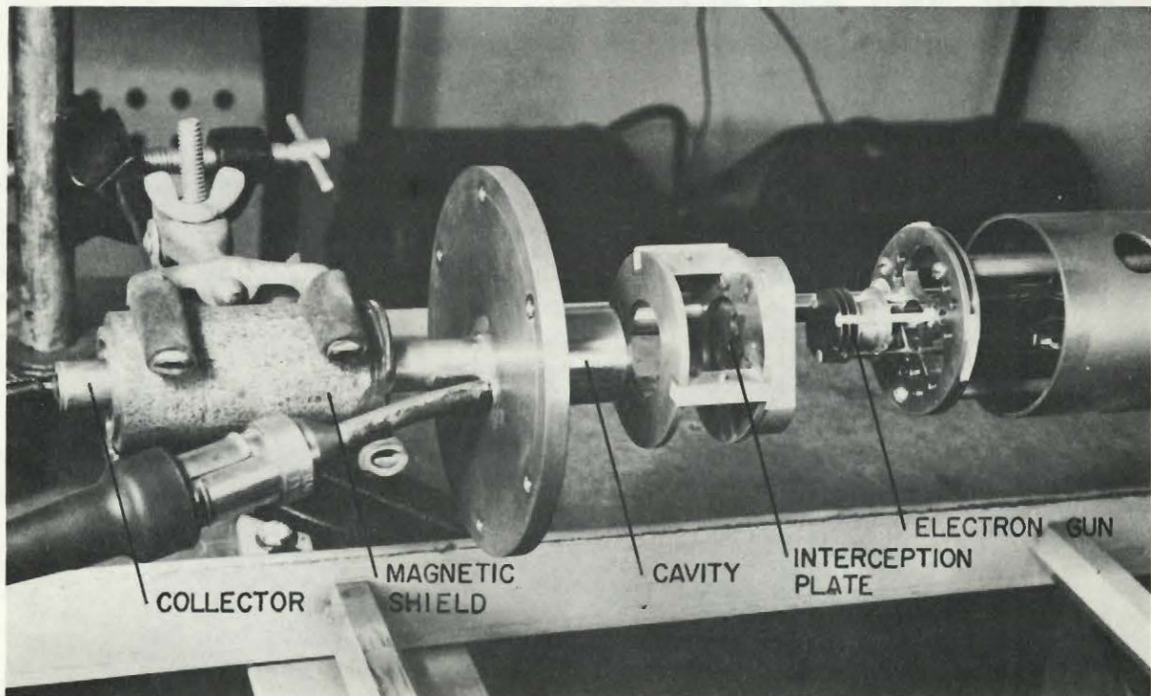


FIG. 3-2 INNER COMPONENTS OF THE TUBE STRUCTURE

grids was mounted perpendicular to the beam axis, the other at an angle of  $20^\circ$  in order to intercept a larger fraction of the beam current. All electrodes were assembled on a single plate which pivoted on the plunger controlling the longitudinal motion. By rotating the plunger, any one of the electrodes could be moved into the path of the beam.

The resonant cavity was a standard re-entrant type with a resonant frequency of 3050 mc/s. Mounted directly behind the cavity, on the outside of the circular brass plate seen in Fig.3-2, is the electron collector. It was surrounded by a soft-iron magnetic shield in order to eliminate the spurious noise caused by reflected secondary electrons passing back through the cavity gap (Kornelson 1957). The details of these structures are shown more clearly in the mechanical drawing of Figure 3-3.

The plungers controlling the motion of the electron gun and interception plate were driven by a variable-speed motor by means of a rack-and-pinion gear system. The arrangement, shown in the photograph of Figure 3-4, was such that either the electron gun or the interception plate could be moved while the other was held fixed; or both could be driven simultaneously with a fixed spacing between them. The vacuum seals which allowed the plungers to slide through the wall of the vacuum chamber employed teflon packing glands. Double glands were used in each seal and the region between glands was exhausted with a small mechanical pump in order to reduce the leak rate. The plunger which moved the interception plate also served to carry the intercepted current since the whole structure was insulated from the ground by the teflon inserts on the sliding frame and by the teflon glands at the sliding seal.

A 3-stage oil diffusion pump, which is partially visible in the left

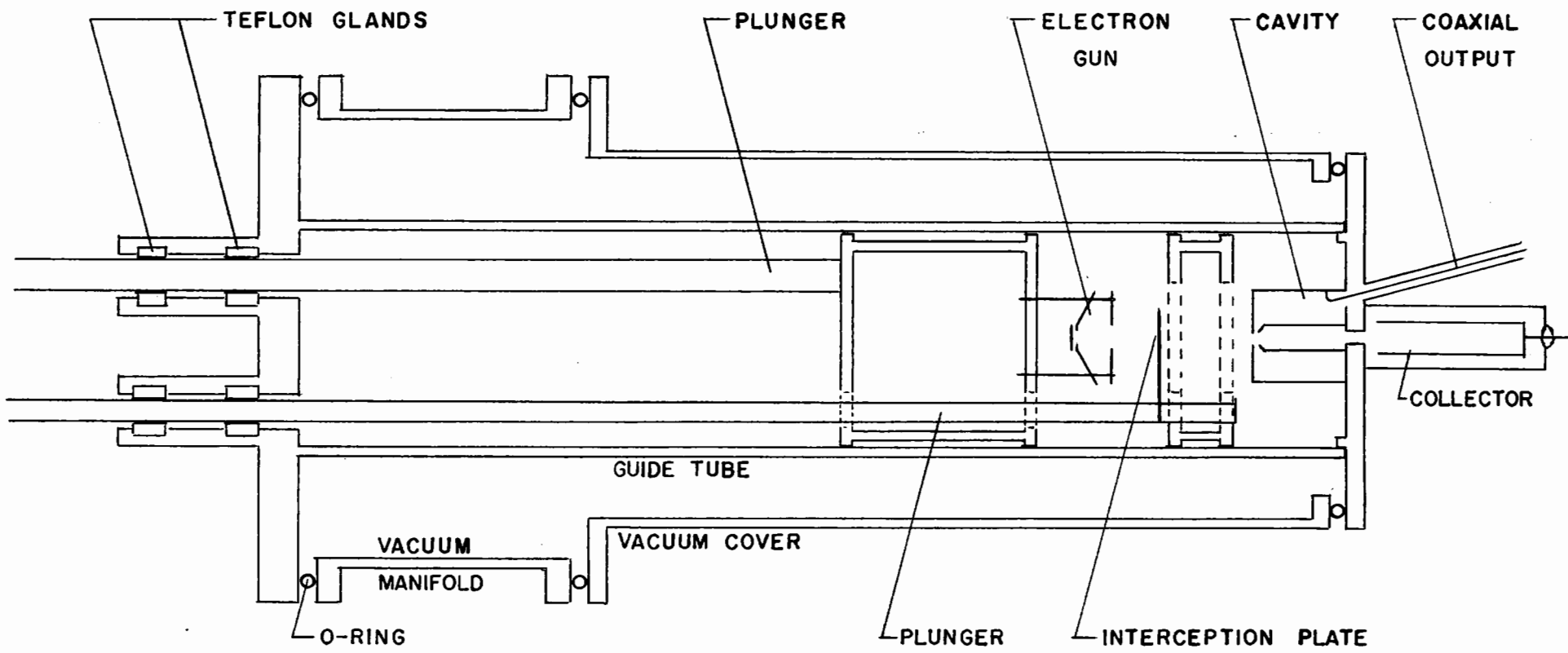


FIGURE 3-3 THE TUBE ASSEMBLY

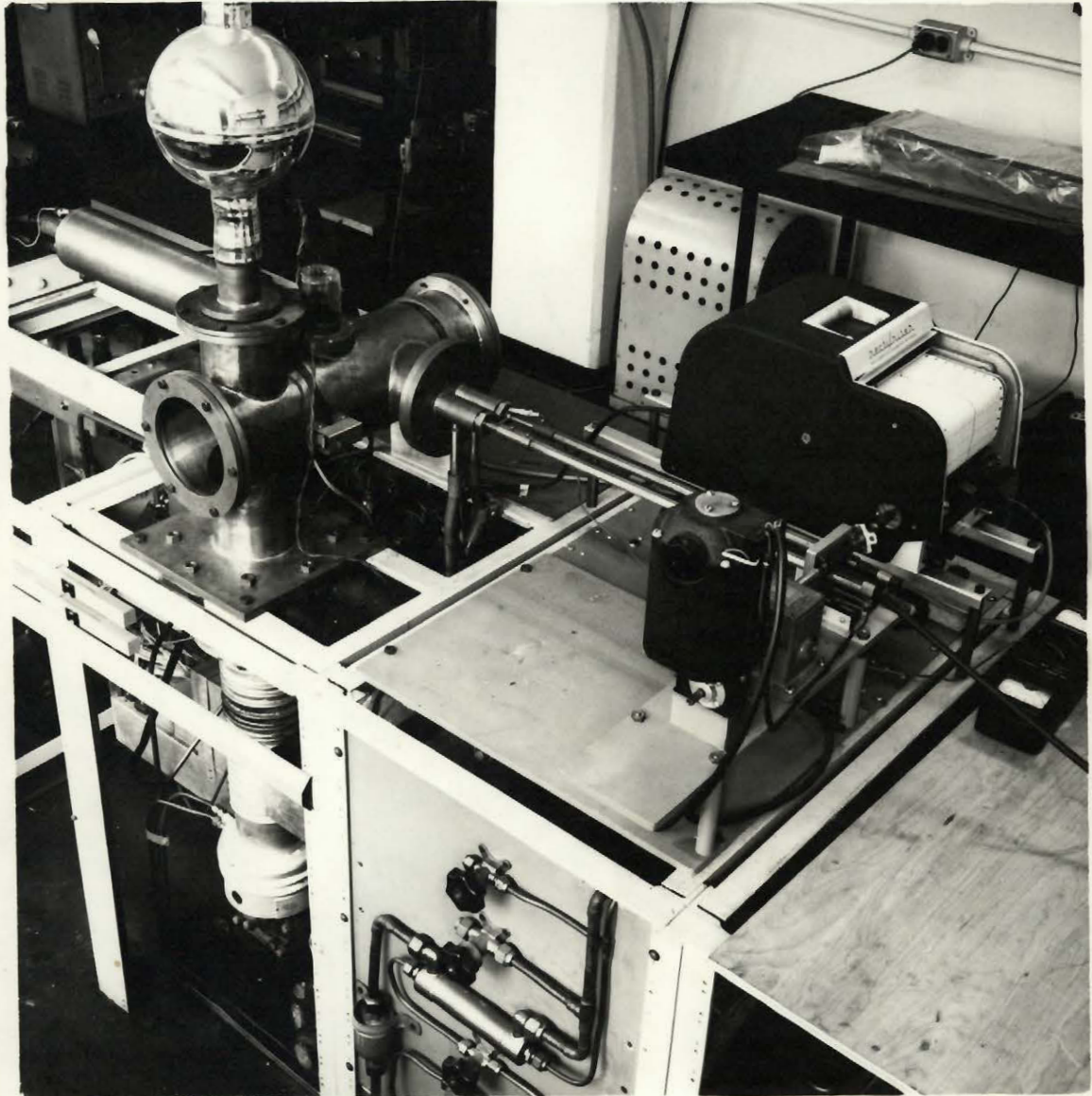


FIG. 3-4 REAR VIEW OF THE APPARATUS

foreground of Figure 3-4, was the main element in the vacuum system. Between the diffusion pump and the vacuum manifold was a baffle which was maintained at a temperature of  $-40^{\circ}\text{C}$  by a Freon refrigeration unit. Pressure in the vacuum chamber was measured by means of a Bayard-Alpert type ionization gauge whose elements projected directly into the vacuum manifold in order to give a true pressure reading. The normal operating pressure of  $3 \times 10^{-6}$  mm of Hg. could be reduced by a factor of ten by means of an auxiliary liquid nitrogen cold trap.

### Electron Guns

The electron gun initially used in the noise measurements followed a design originated by Kornelsen especially for use in demountable vacuum systems. It employed an indirectly heated tantalum emitter which was not subject to contamination at the moderate vacuum ( $10^{-5}$  to  $10^{-6}$  mm Hg) attainable in a demountable system. Nor was it affected by repeated exposure to atmospheric pressure when changes had to be made in the tube structure.

The main elements of the gun are shown in Figure 3-5. Elements A, B and C form the electron gun proper. A and B are beam forming electrodes (anode and cathode respectively) which were shaped according to the theory of Pierce (1949). The emitter C is a circular "button" of tantalum .10" in diameter and .010" thick. From it, three equally spaced arms extend radially to a supporting electrode D. The tantalum button is heated by electron bombardment, the bombarding electron stream being produced by a second electron gun consisting of elements D, E and G. The emitter G was made by winding .005" diameter tungsten wire in the form of a toroidal coil.

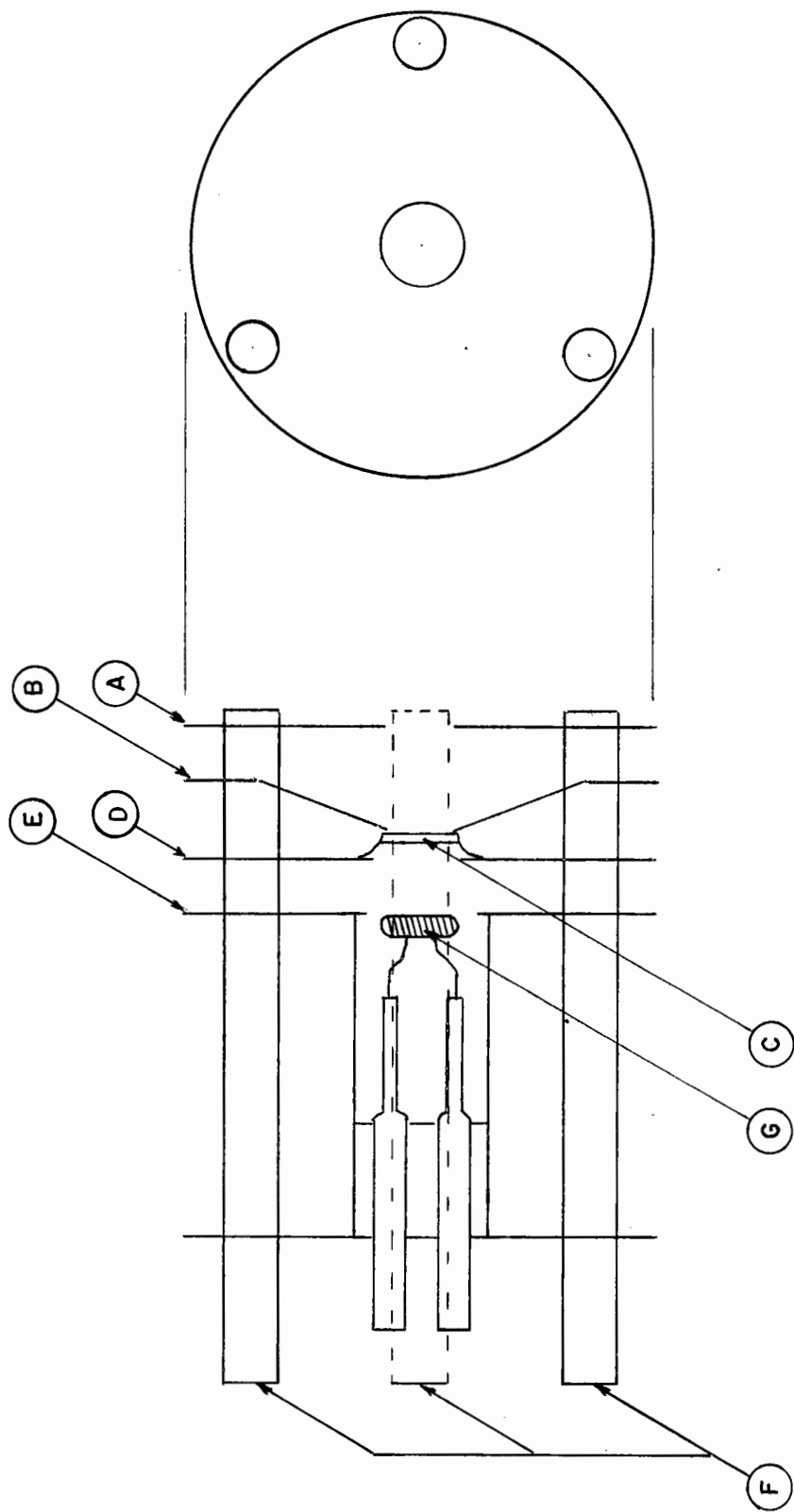


FIGURE 3-5 THE BOMBARDED-CATHODE ELECTRON GUN

Since the emitters C and G are only of the order of .1" in diameter, it was necessary to shape them by hand under a binocular microscope.

Pertinent data on the Pierce-type gun are:

cathode-anode spacing	4.6 mm,
cathode aperture diameter	1.5 mm,
anode aperture diameter	2.4 mm,
measured perveance	
(defined by $G = I_0/V_0^{3/2}$ )	$1.1 \times 10^{-7}$ (amp.)(volt),
cathode temperature for	
space-charge-limited	
emission (Kornelson 1957)	2300°K.

For the bombarding gun:

the cathode-anode voltage was 500 volts;  
the bombarding electron current necessary to  
heat the tantalum button to space-charge  
limited emission was 45 ma.

For measurements of the variation of interception noise with magnetic field strength, an electron gun with an oxide-coated cathode was used since the bombarded-cathode gun did not operate satisfactorily in magnetic fields of less than 700 gauss. At low field strengths the bombarding beam was so divergent that insufficient current was delivered to the tantalum button to achieve space-charge limitation in the primary gun.

Previous attempts in this laboratory to operate an oxide-coated cathode in a demountable vacuum system had been unsuccessful. The primary source of contamination appeared to be the silicone vacuum grease used at O-ring

seals, particularly where sliding seals were necessary. At the suggestion of Professor G. A. Woonton, dry O-rings and teflon sliding seals were used in the author's vacuum system. An oxide-coated cathode was operated in the system at intervals over a period of several weeks. During this time a gradual decrease of cathode activity was noted. However, the noise behaviour was consistent from day to day and showed adequate reproducibility.

The dimensions and measured perveance of the gun were the same as listed previously for the other Pierce-type gun. The cathode temperature necessary to produce space-charge limited emission was 1350°K. This was estimated from curves of cathode temperature versus heater power obtained by Desrocher (1958) for a similar gun.

#### The Measuring System and Electrical Circuits

In discussing the sensitivity of the measuring apparatus used in these experiments, it is necessary to consider the problem of discriminating between random noise from the electron beam (which will be referred to as the "signal") and the background of random noise fluctuations that are inherent in the measuring apparatus itself. Since the spectral density of the electron beam noise is essentially constant over a narrow frequency range, the signal power is proportional to the bandwidth of the microwave cavity (or of the intermediate-frequency amplifier, whichever is the smaller).

The signal changes to be measured are essentially changes in d-c level, or at most, slow variations. Hence considerable improvement in sensitivity can be obtained by narrowing the bandwidth after detection. The fractional fluctuations in signal level, due to receiver noise, are then of the order of

$$\left[ \frac{\text{bandwidth after detection}}{\text{bandwidth before detection (I.F. or R.F.)}} \right]^{\frac{1}{2}}$$

The above factor can be made very small since the bandwidth after detection need only be of the order of cycles per second whereas before detection it will be of the order of megacycles/sec. However, direct-current amplifiers are subject to spurious gain fluctuations so that the indicated increase in sensitivity may not be realized in practice. A method of minimizing gain fluctuations is to modulate the original signal at a low audio frequency and then perform the final detection in a coherent (or synchronous) detector. This method has come to be known as the "Dicke radiometer" technique. (Dicke 1946).

The measuring system is shown in Figure 3-6 and 3-7. The electron beam was gated by a symmetrical square wave at 35 c/s. The microwave cavity was followed by a conventional superheterodyne receiver. The 35 c/s signal detected by the bolometer was amplified by a tuned amplifier (bandwidth  $\approx 2$  c/s) and then detected coherently. The synchronizing signal for the coherent detector was provided by the same square wave used to modulate the electron beam. Following the synchronous detector, the bandwidth was reduced to 0.5 c/s and the output signal applied to a 0-1 ma. linear recorder. In order that recorder readings be maintained greater than half-scale over a wide range of signal levels, attenuation in steps of 3 db was inserted before the synchronous detector.

MacFarlane (1956) has analysed this system and found that the limiting sensitivity is a signal 35 db below the self-noise of the receiver alone. Detection of signals of the order of  $10^{-15}$  watts has been achieved easily.

Since a bolometer is a square-law device, the output of the measuring system (ie., recorder current) was proportional to the noise power output from the cavity. The linearity of the measuring system from the input of

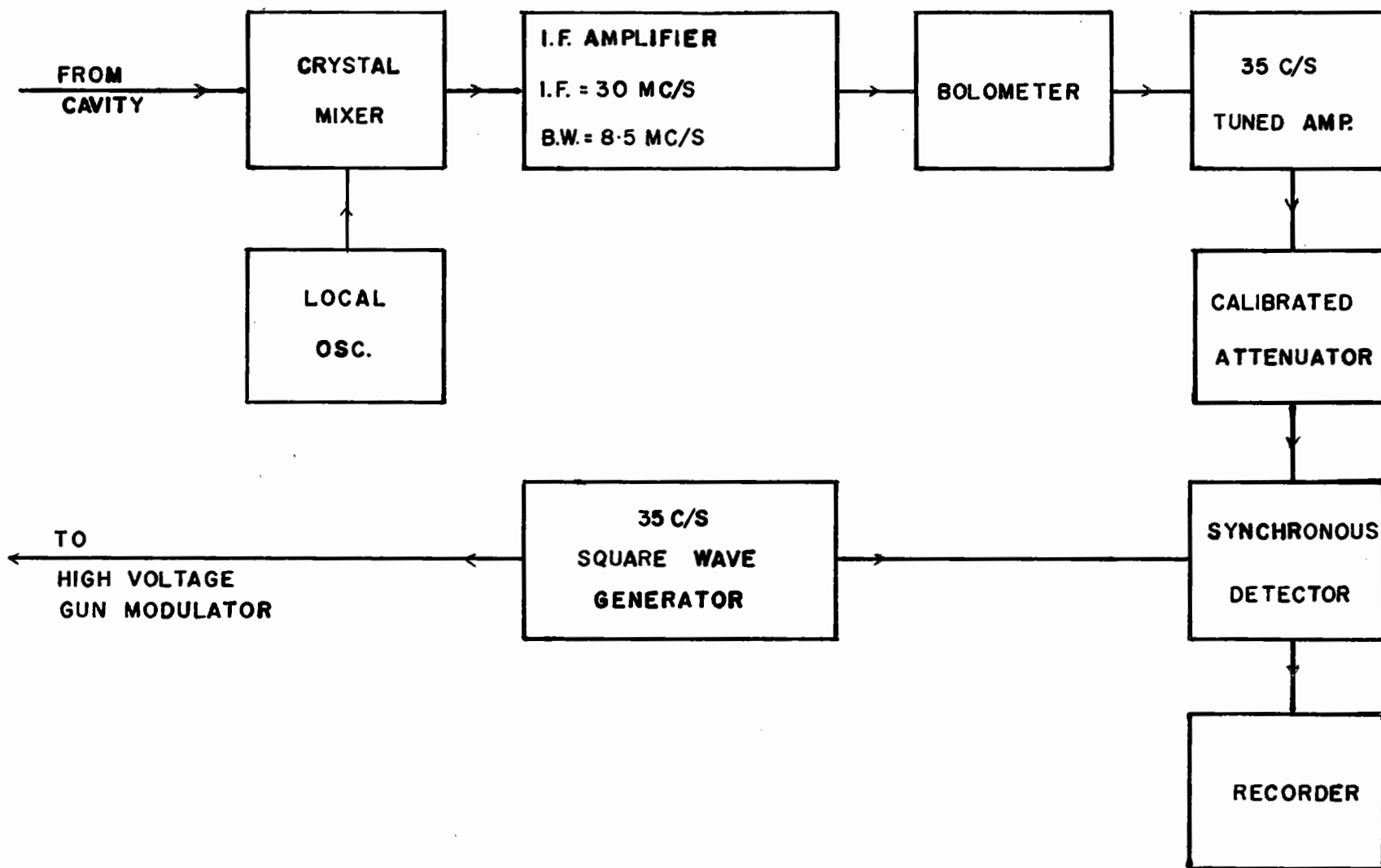


FIGURE 3-6 THE MEASURING SYSTEM

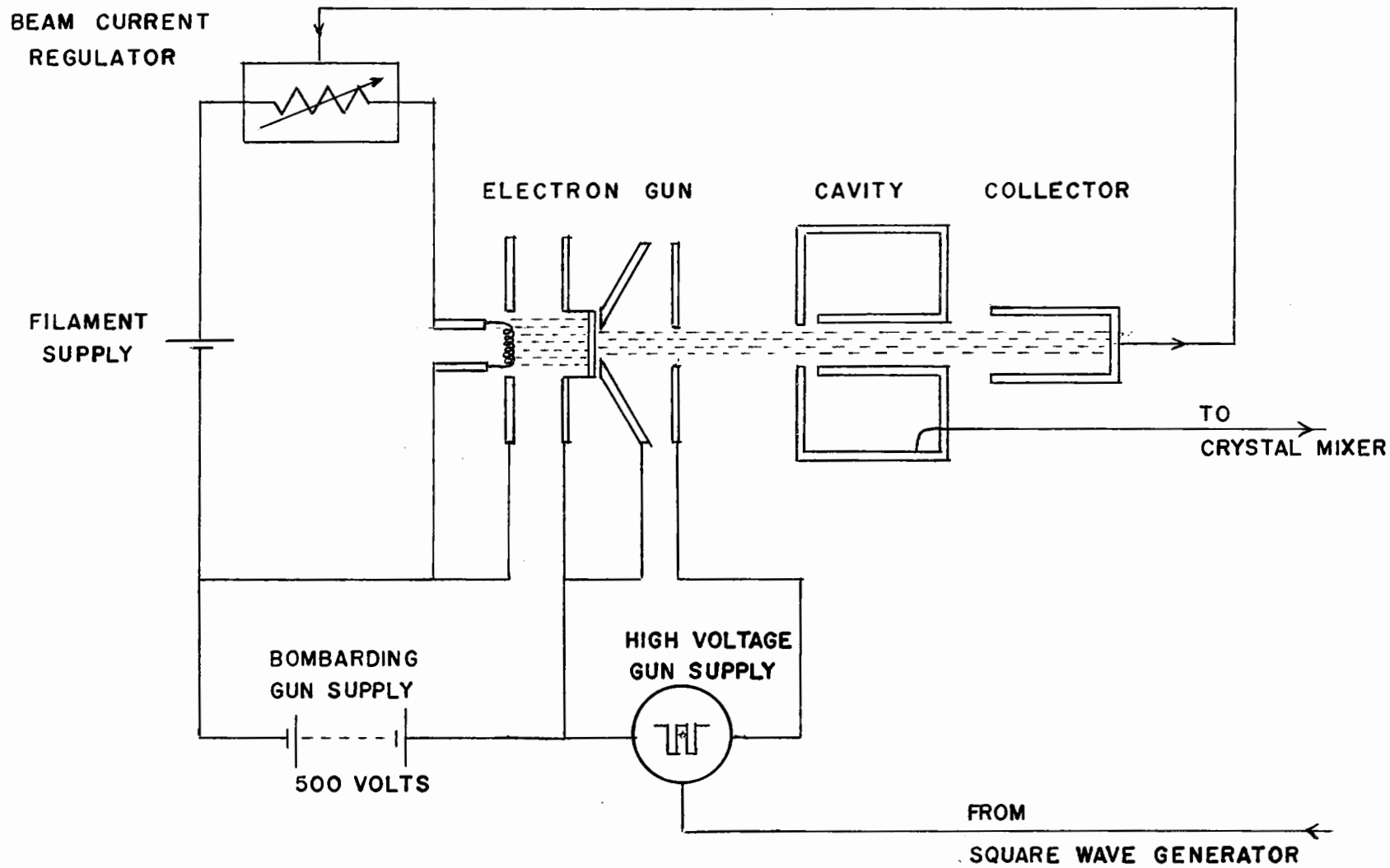


FIGURE 3-7 CIRCUITS ASSOCIATED WITH THE ELECTRON BEAM

the crystal mixer up to and including the recorder was measured by means of a calibrated signal generator. Output readings were found to be linearly related to power input to within  $\pm 0.2$  db over a dynamic range of 25 db. It must be noted that the measurement of linear dynamic range with a signal generator is not a good criterion for a noise measuring system, since for r.m.s. noise power equal to the maximum tolerable signal power, there will be noise peaks which extend well into the non-linear region. However, in operating the measuring system, the gain was adjusted so that the maximum output signal was always 6 to 10 db below the beginning of the non-linear region. Since the gain control was in the early stages of the intermediate-frequency amplifier, it is believed that there was no possibility of saturation on noise peaks.

Figure 3-7 shows in some detail the electrical connections to the bombarded-cathode type of electron gun. It was found necessary to stabilize the electron beam current in the region of temperature limited emission. This was accomplished by a negative-feedback system developed by Kornelsen (1957) in which the collector current controlled the magnitude of a resistance in series with the filament supply for the bombarding gun. Current control by this stabilizer was adequate down to 5 microamperes of beam current. Manual control was necessary for currents below 5 microamperes.

Circuits for the oxide-cathode type of gun consisted only of the high voltage modulator and a cathode heater supply.

Collector current was measured with a meter whose accuracy was known to be better than 1% of full scale. All other voltages and currents associated with the electron beam were monitored with meters of 5% accuracy.

CHAPTER 4

MEASUREMENTS

In the first series of measurements for which the apparatus was used, the interception plate and the cavity were located at the anode of the electron gun. Noise smoothing, before and after interception by the various electrodes, was obtained as a function of electron gun voltage at a fixed value of magnetic field strength. The variation of smoothing with magnetic field strength was measured for a constant value of gun voltage.

The investigation of the effect of interception on the noise space-charge waves in the drift space consisted in measurements of noise power as the electron gun was moved back from the cavity, with the interception plate at various positions between gun and cavity. These measurements were carried out for the condition of space-charge-limited emission and for temperature-limited emission.

I Calibration of the Measuring System

The apparatus was calibrated by a method used by Cutler and Quate (1950). With the cavity at the anode of the electron gun, relative noise power was measured as the beam current was increased from zero to its maximum value at space-charge limitation. Typical curves of noise power versus collector current which resulted from measurements using the bombarded-cathode gun are shown in Figure 4-1. In the region of temperature-limited current the noise power rose linearly with collector current as predicted theoretically by the shot-noise relation,

$$\overline{i_n^2} = 2e I_0 \Delta f.$$

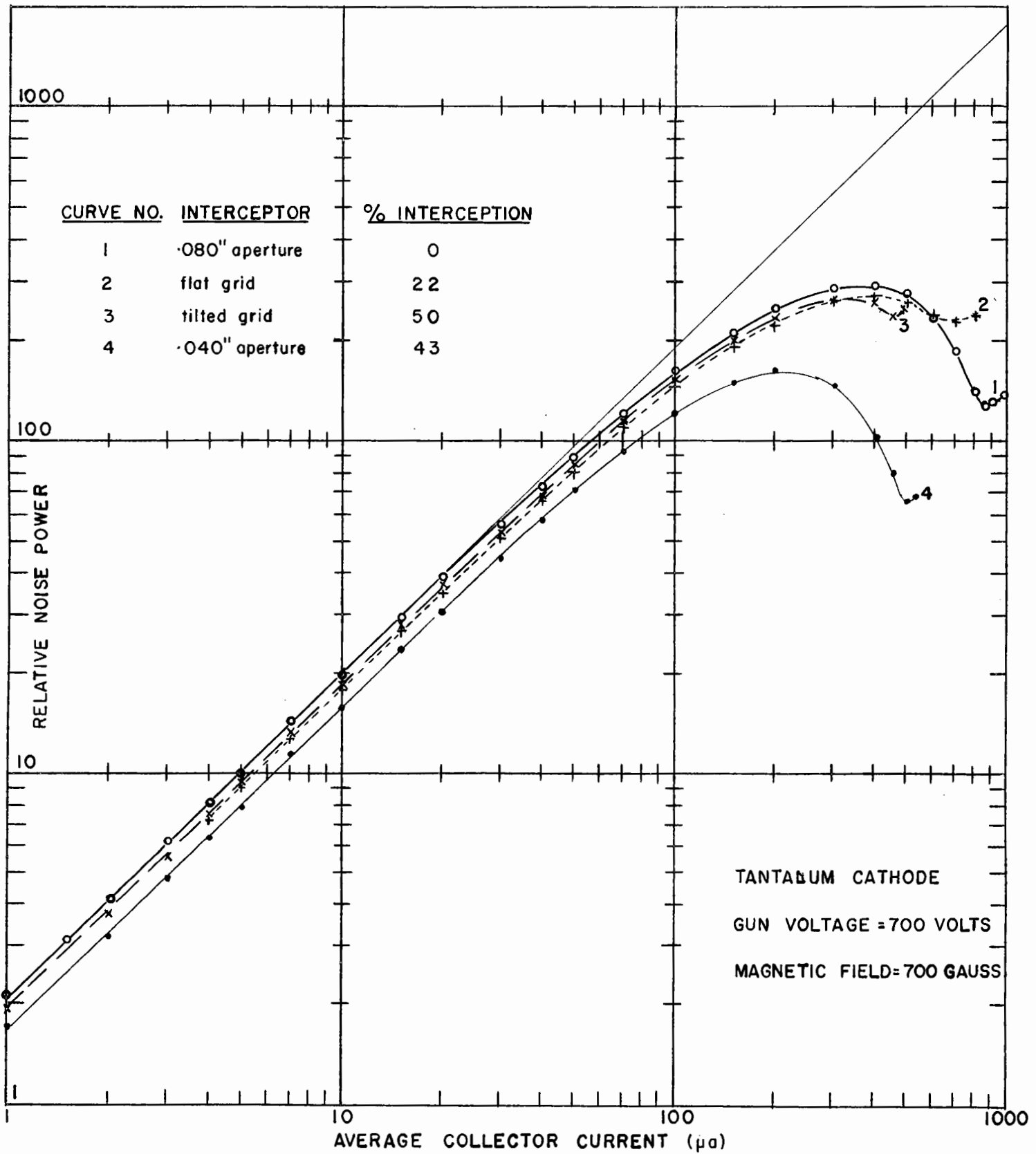


FIGURE 4-1 VARIATION OF NOISE POWER WITH COLLECTOR CURRENT

The onset of smoothing, as the cathode temperature was increased further, may be clearly seen from the curves. At the maximum value of space-charge-limited current, the ratio of measured noise power to the equivalent shot-noise power determined by extrapolating the linear portion of the curve to the same current yields the smoothing factor  $\Gamma^2$ .

The value of collector current at which  $\Gamma^2$  was determined was to a certain extent arbitrary. In the electron gun, the transition from temperature-limited emission to space-charge-limited emission is a gradual one. There is no precise value of current which may be said to be the "space-charge-limited point". As may be seen from Figure 4-1, the relative noise power reached a minimum in the region of space-charge-limited emission, and then began to increase again with increasing current. This effect was most pronounced at low gun voltages. For example, at 200 volts, the noise reached a minimum at  $I_0 = 135 \mu$  amperes, then increased continuously to  $I_0 = 240 \mu$  amperes. The latter current was the maximum value attainable with reasonable safety to the cathode. In many cases the noise rose nearly parallel to the shot-noise asymptote; i.e., the smoothing was constant. This behaviour was not consistent for different gun voltages.

Zero-interception smoothing was measured at the maximum value of beam current attained for each gun voltage. Similarly, for the various fractions of interception, the smoothing was measured when this maximum value of incident current was obtained.

Measurements of the variation of interception noise with magnetic field strength was normalized to shot noise by means of smoothing curves obtained for a fixed value of magnetic field. Similarly, in the case of measurement of noise space-charge waves along the electron beam, the relative noise

power levels of the maxima and minima were referred to the level at the anode which had been determined with respect to shot noise from the smoothing measurements.

## II Precision and Accuracy of Measurements

In order to achieve maximum precision in the determination of the smoothing factor  $\Gamma^2$ , it was necessary to obtain a complete smoothing curve for each of the intercepting electrodes and for each value of gun voltage. The reasons for this are the following. The measuring system was subject to slight gain changes over periods of several days. This was the cause of the slight differences in level of the straight-line portion of curves 1, 2 and 3 in Figure 4-1. In the case of the .040" aperture, curve 4, there was a real decrease in power due to the reduced beam diameter and consequent decreased coupling to the cavity. A further effect of beam-to-cavity coupling was the decrease of coupled power with decreasing gun voltage, which was due to the increased transit time across the cavity gap.

An unexpected result from the experimental measurements was that the slope of the shot-noise asymptote (viz. the slope on a log-log plot of the linear portion of the curves shown in Figure 4-1) was less than unity in some cases. That is, at very small values of beam current, noise power was proportional to  $I_0^n$  where  $n$  ranged from 1.0 to about 0.9 depending on gun voltage. In Table 4-I are listed some values of  $n$  obtained by fitting the points on the asymptote to a straight line by the least-squares method. Column three of the table gives the "standard error of estimate" (root-mean-square deviation) in decibels.

TABLE 4-I

Slope of the shot-noise asymptote as a function of gun voltage.

<u>Gun Voltage</u>	<u>Slope "n"</u>	<u>Error of fit, in decibels</u>
1000	0.996	0.04
	1.008	0.05
	1.014	0.2
700	0.992	0.07
	0.992	0.02
500	0.976	0.03
	0.982	0.05
300	0.944	0.02
	0.938	0.06

In a number of other cases, for which least-squares fitting was not carried out, slopes were estimated visually and agreed with the above values to within 1%. At 200 volts the scatter of measured points for low values of collector current became large because of poor signal-to-noise ratio and instability of beam current. The slope was estimated visually as 0.9.

It has been difficult to decide whether the experimental points represent a straight line of non-unity slope or a gradual curve which might asymptotically approach a line of unity slope at much lower currents. Visual examination of a large number of sets of points, and the smallness of the r.m.s. deviations listed in Table 4-I have led the author to assume that a straight line of non-unity slope is the correct interpretation.

Similar smoothing measurements carried out by McFarlane (1958) in this laboratory on two "sealed-off" tubes showed a similar range of slope with gun voltage. These measurements were made at a frequency of 4,200 mc/s and with no confining magnetic field. On the other hand, McFarlane has obtained unity slope with similar tubes at frequencies of 1,400 mc/s and

9,500 mc/s.

Careful examination of the linearity of the measuring system and its overall stability has ruled out these as possible causes of the observed non-unity slopes. Although the evidence is not conclusive, the most probable explanation lies in the non-uniformity of coupling between the electron beam and the cavity. This matter is dealt with in more detail in Appendix 2.

Values of  $\Gamma^2$  then, have been calculated from the extrapolated straight-line portion of the smoothing curves. An upper limit on the possible error in the values of  $\Gamma^2$  has been assessed as follows:

from determination of the noise power at the maximum  
current point, taking into account graphical smoothing  
-----  $\pm 0.1$  db; from determination of the shot-noise  
asymptote using a least-squares fit -----  $\pm 0.1$  db;  
total possible error -----  $\pm 0.2$  db.

This is believed to be a reasonable estimate at the higher gun voltages: 500, 700, 1000 volts. From inspection of several sets of data, the author has been led to assign larger errors,  $\pm 0.5$  db and  $\pm 1$  db at gun voltages of 300 and 200 volts respectively.

### III Space-Charge Wave Measurements

For these measurements the chart recorder was driven externally in synchronism with the motion of the electron gun. A typical record is shown in Figure 4-2. The smooth pattern of the curve is broken near the minima by changes in the relative gain of the measuring system. The levels of the minima were recorded at greater than half-scale deflection.

In the case of zero interception, the reproducibility was better than

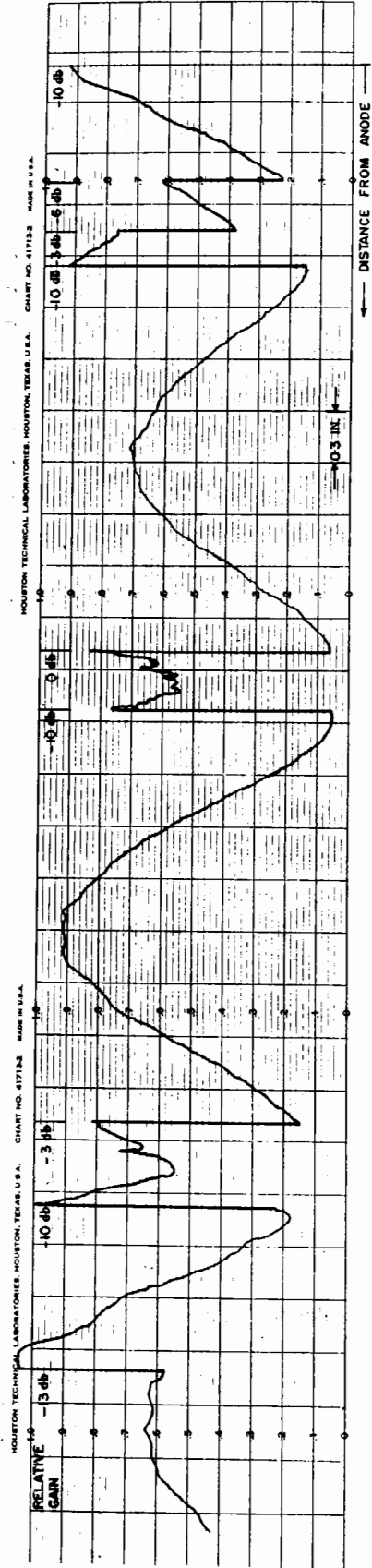


FIG. 4-2 A TYPICAL SPACE-CHARGE WAVE PATTERN

0.5 db for all maxima and the first minimum. The scatter of points at the second and third minima for seven records of the zero-interception wave is shown in Figure 4-3. It is believed that these fluctuations were due to secondary electrons or to d-c beam perturbations.

The serious deterioration of smoothing caused by electrons reflected from the collector and returning through the cavity gap has been described by Vessot (1957) and Kornelsen (1957). The precautions taken to eliminate effects of secondary electrons have been discussed in Chapter 3. When the electron gun was stopped at a minimum of the noise standing wave, it was found that the noise level was sensitive to slight changes in the orientation of the magnetic shield surrounding the collector. Both size and position of the shield were adjusted to minimize the noise level, but it was impossible to say whether all reflected electrons had been eliminated. It should be noted that the smoothing, at the second minimum for example, was of the order of -26 db ( $\Gamma^2 \sim \frac{1}{400}$ ), so that the introduction of only 0.25% random current would cause a 3 db increase in the noise.

The existence of finite minima in the space-charge wave has been shown theoretically by many authors. (Pierce 1954; Robinson 1954, for example). The theory predicts that the product of the maximum and minimum values of noise power in the standing wave is constant. Referred to shot-noise the relation is,

$$\Gamma_{\max}^2 \Gamma_{\min}^2 = \frac{1}{2} \frac{\omega}{\omega_q} \left( \frac{kT_c}{eV_0} \right)^2$$

The value of this expression for the 700 volt case of Fig. 4-3 is  $\sim -48$  db. The experimental value is only -35 db.

In a practical electron beam, d-c perturbations alone are of sufficient

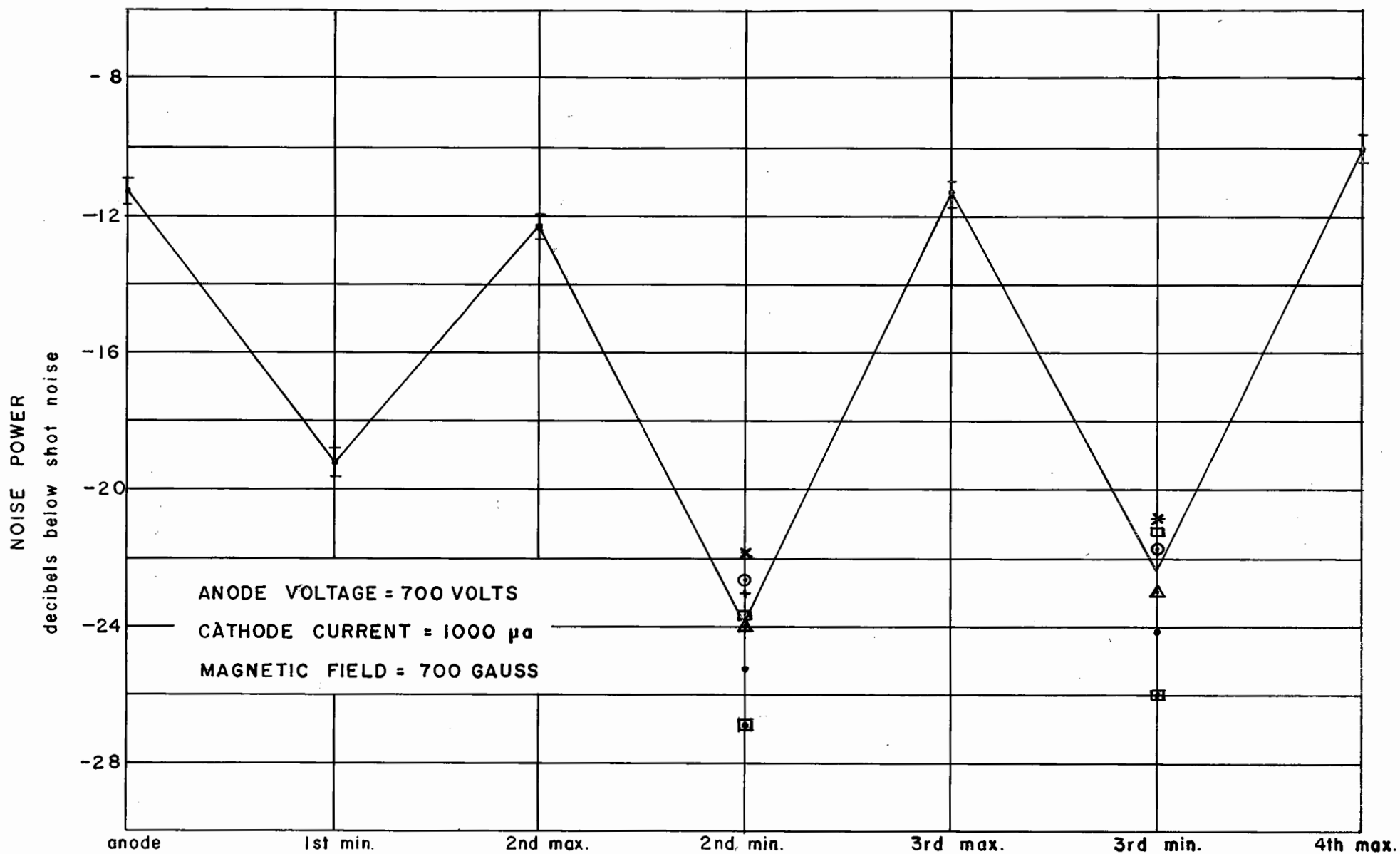


FIGURE 4-3 MAXIMA AND MINIMA OF NOISE IN THE DRIFT SPACE FOR ZERO INTERCEPTION

magnitude to account for finite minima. The space-charge wavelength  $\lambda_q$  is a function of current density which in a practical electron beam varies both with radial and with axial coordinates. A current fluctuation associated with a particular value of radius propagates with a different space-charge wavelength than that at some other radius. There is some average wavelength which can be assigned to the beam, but at a plane where fluctuations propagating with the average wavelength go to zero, the cavity will still respond to the non-zero fluctuations associated with slightly different wavelengths.

The space-charge wave for zero interception shown in Figure 4-3 also exhibited two features which have been noted by other workers (Rowe 1952, Kornelson 1957, Shkarofsky 1957). These were, (1) the gradual rise of the levels of the maxima and minima with distance, and (2) the fact that the first minimum was always higher than the second, and the second maximum was always lower than all others. Although these phenomena are not thoroughly understood, the first is usually attributed to an increase in noise due to electron-molecule collisions, and the second due to the strong excitation of higher order modes.

CHAPTER 5

Experimental Results and Their Interpretation

I Interception Noise as a Function of Magnetic Field Strength

The measurements to be described here were made with the emission from the oxide-coated cathode space-charge limited at an anode voltage of 700 volts.

Figure 5-1 shows the measured values of beam noise after interception as a function of the strength of the confining magnetic field. Ordinate values represent the noise content of the transmitted beam normalized to full shot noise in the transmitted current. In the case of the circular apertures, the amount of current transmitted was a strong function of the value of the magnetic field. The number associated with each experimental point in Figure 5-1 is the percent transmission at that field strength. As noted on the graph, the transmission factor of the grids was independent of magnetic field strength.

The striking difference between the amount of noise added to the beam by grid interception and that added by aperture interception is evident from these measurements. For comparable fractions of current intercepted, the magnitude of  $\Gamma_2^2$  is from 3 to 6 db less from grid interception than for aperture interception. The experimental points of curve D for the .060" aperture are particularly significant in the region from 350 gauss to 700 gauss. Here the interception varied from 3% at 700 gauss to 20% at 350 gauss, but the decrease in smoothing from the zero-interception value of approximately 14 db was less than 0.5 db.

For the purpose of comparison with theory the predicted values of  $\Gamma_2^2$

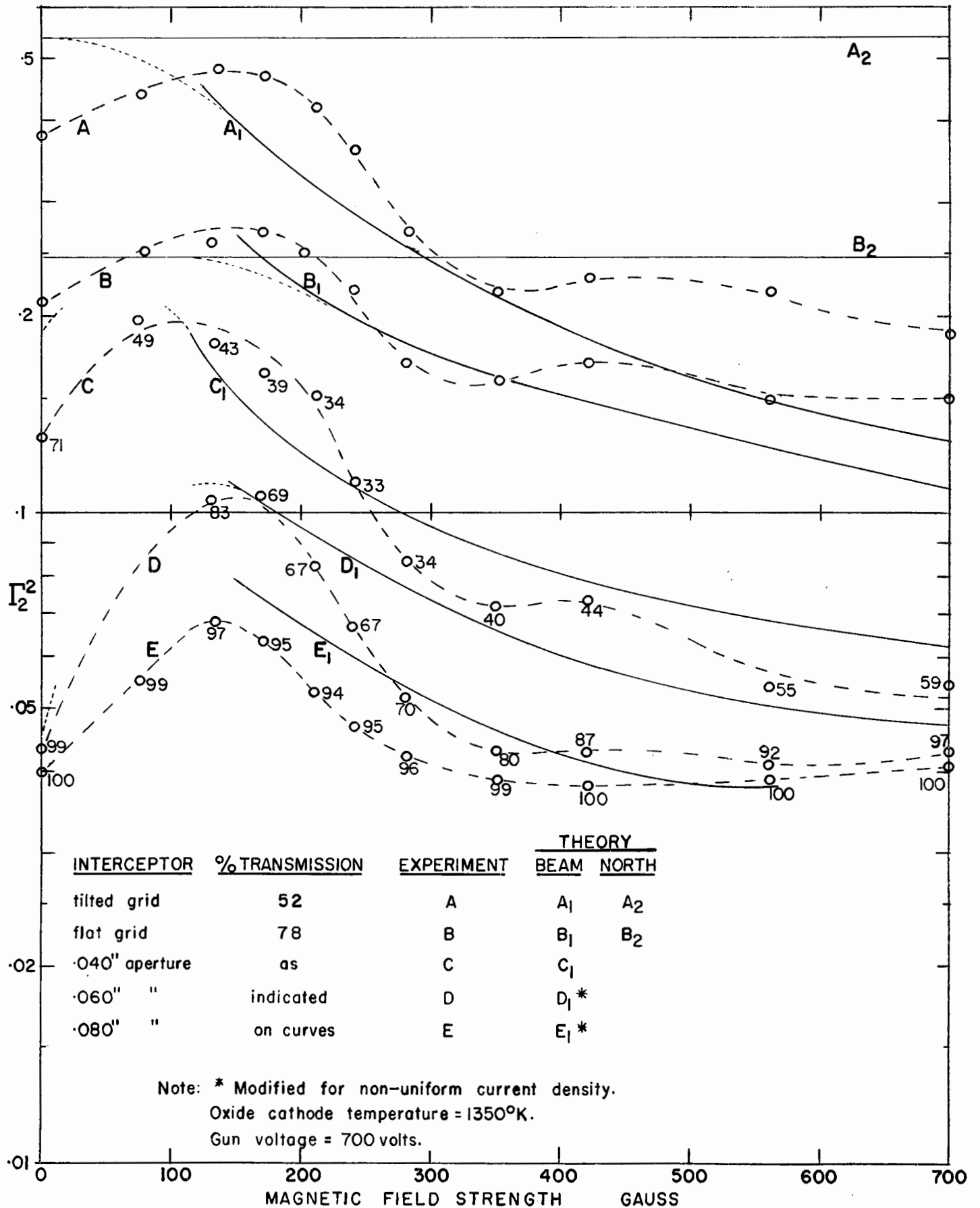


FIG. 5-1 NOISE SMOOTHING AS A FUNCTION OF THE CONFINING MAGNETIC FIELD

given by

$$\Gamma_2^2 = \Gamma_1^2 + (1 - \Gamma_1^2) \frac{\Omega_2}{\Omega_1}$$

has been plotted on the graph for each of the intercepting electrodes. The details of the calculation of  $\frac{\Omega_2}{\Omega_1}$  for particular electrode geometries are given in Appendix I, section II.

The measured values of  $\Gamma_2^2$  are in qualitative agreement with the functional variation predicted by the theory of Beam for magnetic field strengths greater than 150 gauss. That is, the noise decreased with increasing magnetic field strength. The smaller undulations in the experimental curves are thought to have resulted from scalloping on the beam since they were found to be consistent with variation of scallop wavelength  $\lambda_s$  of the form

$$\lambda_s \propto \frac{(\text{beam voltage})^{\frac{1}{2}}}{\text{magnetic field strength}}$$

The magnitude of the smoothing measured for the flat grid and for the .040" aperture lies within 1 db of the predicted value over the range 100 to 700 gauss. The theoretical smoothing is consistently low in the case of the tilted grid, and high for the larger apertures. In the latter cases, the use of the modified current density as given in Equation (2-25) has slightly improved the agreement between theory and experiment. In the practical electron beam the current density profile is frequently more non-uniform than predicted by theory. This has been shown by the experiments of Ashkin (1957) and of Cutler and Saloom (1955).

Some idea of the radial variation of current density of the beam used in the author's experiments may be gained by examining the figures for percent transmission by the three apertures at constant magnetic field strength.

If the current density is reasonably uniform, the effective beam radius  $r_b$  is given by  $\left(\frac{r_a}{r_b}\right)^2 =$  fraction of current transmitted, provided the interception is large. The .040" and .060" apertures yield "effective" beam radii of 0.79 mm and 0.84 mm respectively. Theory predicts that the interception will have dropped to 1% for an aperture with radius 2% greater than the "effective" beam radius. Experimentally, 1% of the current is intercepted by the .080" aperture the radius of which is roughly 20% greater than the calculated effective beam radius. Thus the direct current density in the actual beam decreased much more slowly than is predicted by theory. This may account in part for the discrepancy between the observed and predicted values of interception noise in cases where the beam is intercepted near the edge.

Concerning the magnitude of the interception noise produced by the mesh grids, it is interesting to note that for field strengths in the neighbourhood of 150 gauss the noise approaches or exceeds the North values plotted as curves  $A_2$  and  $B_2$  in Figure 5-1. At these values of magnetic field, the theoretical mean spreading radius is nearly equal to the radius of one grid module. In the actual physical beam, small d-c perturbations in the electron gun, probably increase the spreading radius. Hence it would be expected from the theoretical agreements of Chapter 2 that the noise should approach the North value.

The increase in the mean spreading radius, due to transverse velocity other than that of thermal origin, is believed to account for the fact<sup>t</sup> that, for strong magnetic fields, the experimental values of  $\Gamma_2^2$  for the grids are higher than the theoretical values. That this effect should be the more pronounced the finer the mesh of the grid is confirmed by the measurements.

In the case of interception by apertures, it is to be expected also that an increase in the mean spreading radius would cause increased noise; but the effect of non-uniform current density in reducing noise is believed to be larger. Evidence will be presented later, when interception noise on a temperature-limited beam is discussed, to show that excess transverse velocity can cause a large increase in the noise produced by aperture interception.

From Figure 5-1 it may be seen that the experimental values of  $\Gamma_2^2$  for each of the intercepting electrodes decreased as the strength of the magnetic field decreased from about 150 gauss to zero. This is a region of transition from a mean spreading radius determined by the magnetic field to a mean spreading radius determined by transit time across the gun. The values of  $\Gamma_2^2$  predicted from transit time considerations are in qualitative agreement with the experimental measurements, but are in error by 1.5 db for the tilted grid and the .040" aperture.

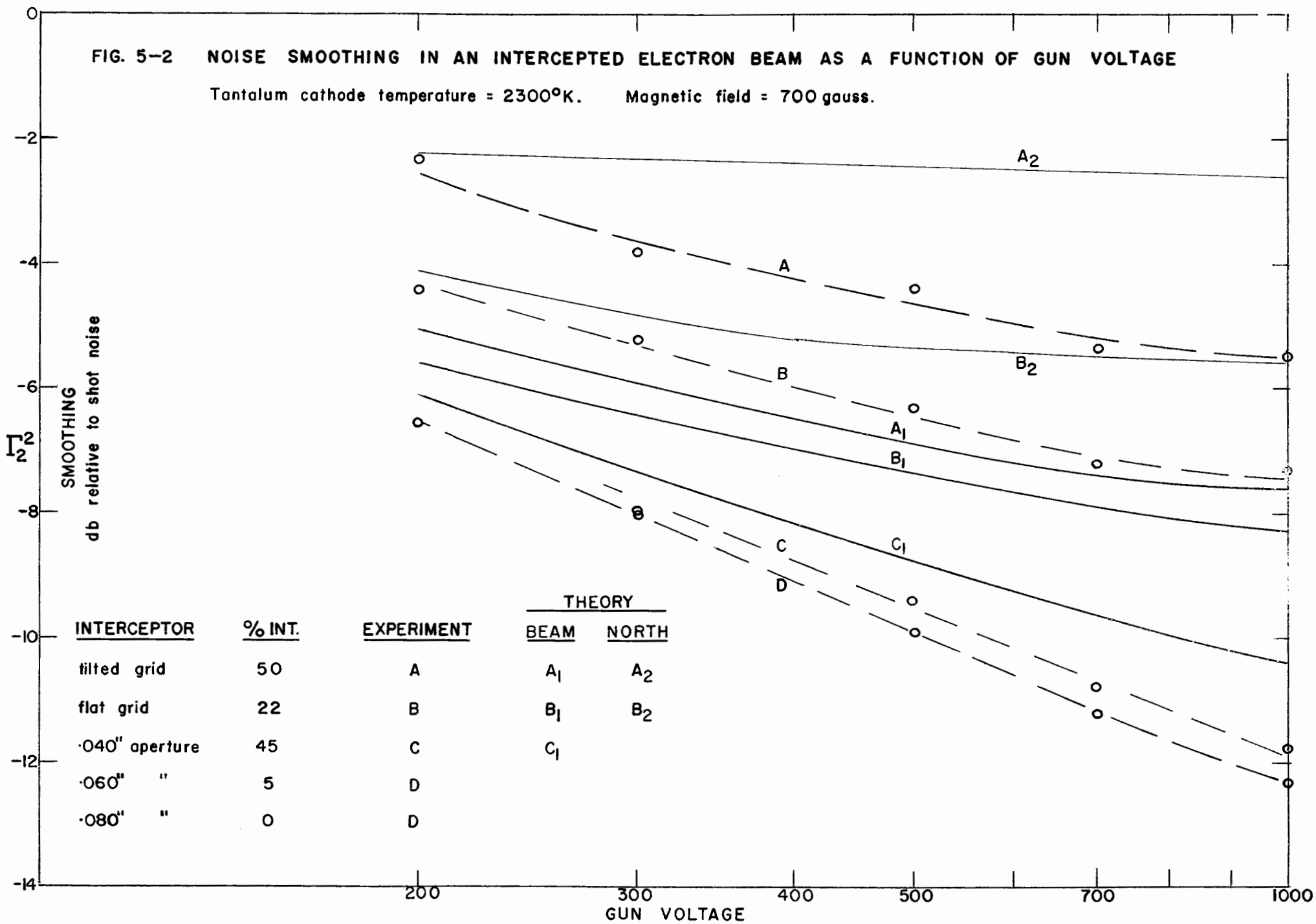
## II The Variation of Interception Noise with Gun Voltage

The significant conditions of the experiment were: interception plate and cavity at the anode of the tantalum-cathode gun, magnetic field constant at 700 gauss. Figure 5-2 shows the collected results of smoothing measurements, similar to those indicated in Figure 4-1, for gun voltages from 200 volts to 1000 volts. The small amount of excess noise caused by aperture interception is again apparent. For five percent interception by the .060" aperture, no change in smoothing was detectable within the precision of the measurements. The .040" aperture which intercepted forty five percent of the beam current caused less than 0.5 db decrease in smoothing.

The results of a comparison of the experimental values of  $\Gamma_2^2$  with

FIG. 5-2 NOISE SMOOTHING IN AN INTERCEPTED ELECTRON BEAM AS A FUNCTION OF GUN VOLTAGE

Tantalum cathode temperature = 2300°K. Magnetic field = 700 gauss.



INTERCEPTOR	% INT.	EXPERIMENT	THEORY	
			BEAM	NORTH
filited grid	50	A	A <sub>1</sub>	A <sub>2</sub>
flat grid	22	B	B <sub>1</sub>	B <sub>2</sub>
.040" aperture	45	C	C <sub>1</sub>	
.060" "	5	D		
.080" "	0	D		

the values predicted by the theories of Beam and North are not significantly different from those of the previous section. The theoretical smoothing predicted by Beam's theory is roughly 1 db lower than the experimental curve for the flat grid and 2 db lower for the tilted grid. These differences are approximately constant over the range of gun voltage from 200 volts to 1000 volts.

If, as conjectured in the previous section, the discrepancy between the experimental and the theoretical values of smoothing for interception by the grids is due to excess transverse velocity caused by imperfect focusing in the gun, it might be expected that the focussing defect would be relatively more severe when the accelerating potential in the gun is low. This conclusion is supported by the fact that the experimental values for the grids are within 0.4 db of the values predicted by North's theory at a gun voltage of 200 volts, whereas the deviation from the North value is as much as 3 db at 1000 volts. The experimental curve for the flat grid, in particular, appears to approach the North value asymptotically at low gun voltages.

### III Space-Charge Waves on an Intercepted Beam

#### (1) Space-Charge Limited Emission

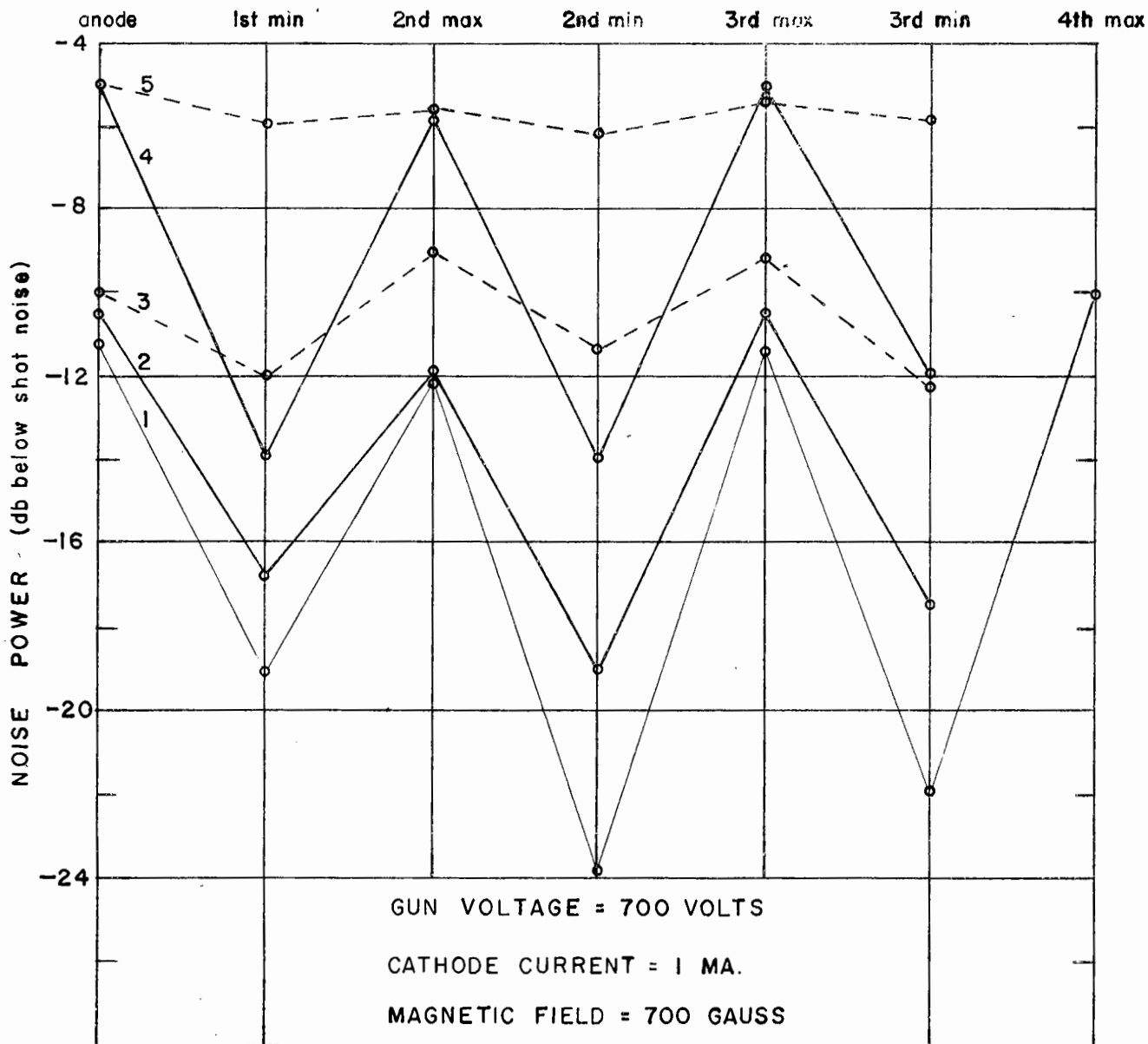
Using the tilted grid and the .040" aperture as intercepting electrodes, noise was measured as the electron gun was moved away from the cavity. This was done for two cases: first, with the intercepting electrode at, and moving with, the anode of the electron gun; second, with the intercepting electrode stationary at the cavity.

Figures 4-3 and 5-4 show the maxima and minima of the noise space-charge

waves for gun voltages of 700 and 1000 volts, respectively. Ordinate values are  $\Gamma_2^2$  = noise power relative to full shot noise in the transmitted current. It is to be emphasized that this graphical representation of the levels of the maxima and minima does not show the complete form of the space-charge waves, nor the fact that the wavelength is different in each case.

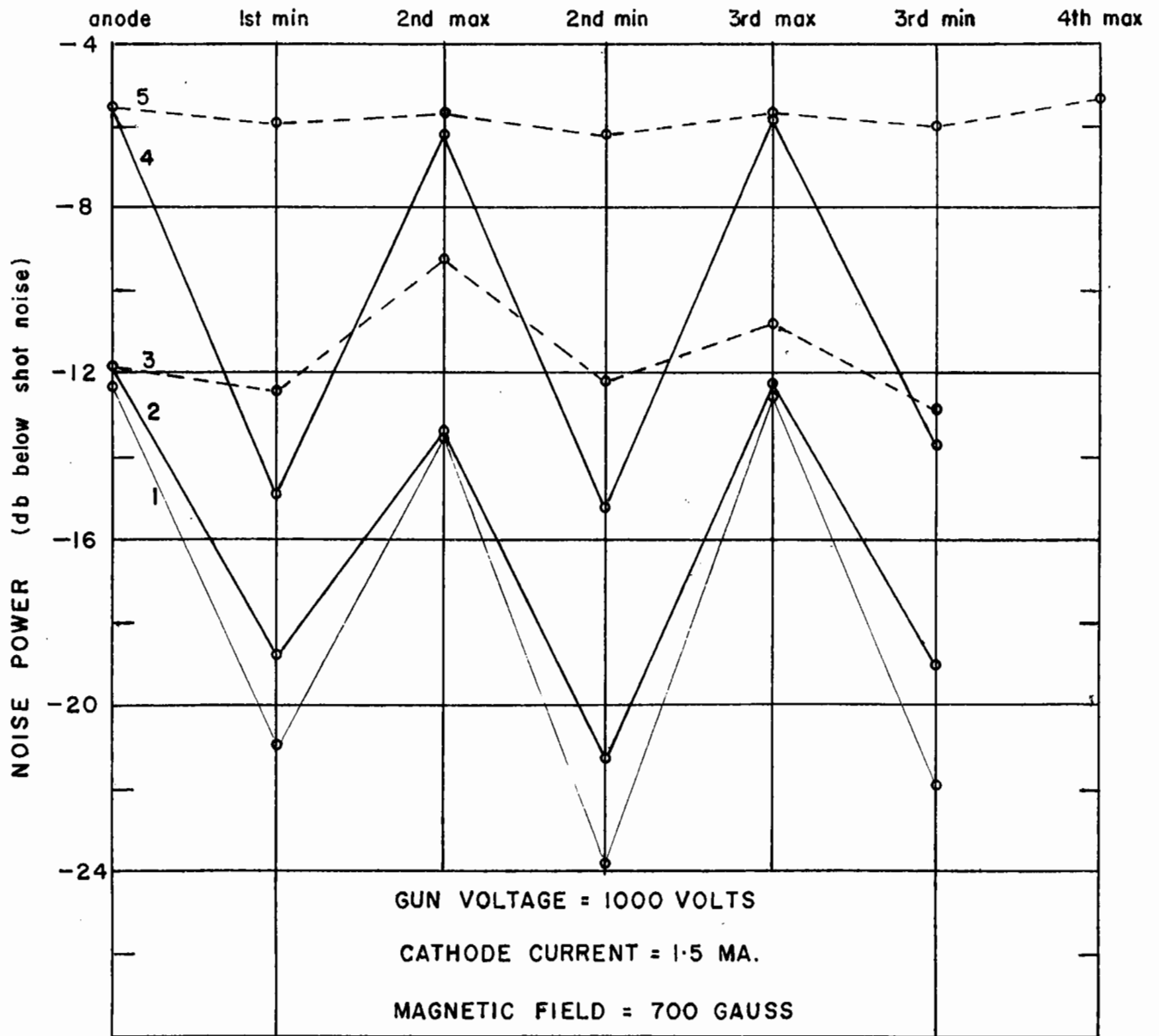
The .040" aperture, intercepting 50% of the beam current at the anode (curve 2), had only a small effect on the space-charge wave. The level of the minima was increased by approximately 2 to 4 db in 20 db. In the case of grid interception at the anode (curve 4), the overall noise level was much higher, but the ratio of maximum power to minimum power was still large. The standing-wave ratio was, in fact, greater than that for the first minimum of the unintercepted beam (curve 1).

When the beam was intercepted at the cavity (curves 3 and 5), the standing-wave ratio was greatly reduced. With the tilted grid at the cavity, the standing-wave ratio was of the order of 0.5 db as compared with 10 db for the grid at the anode. The analysis of measurements made with the aperture at the cavity was made difficult by the fact that scallops on the beam caused large variations, periodic with distance at the "cyclotron" wavelength, in the fraction of current intercepted. The resulting fluctuations in the noise wave were due partially to changes in the transmitted current and partially to the resulting variation in interception noise. The values of noise power at the maxima and minima were averaged over the scallop fluctuations. The second and third maxima (curve 3, Figures 5-3 and 5-4) showed an appreciable increase over the noise level at the anode. However, this is not considered significant as far as interception noise is concerned, since the d-c perturbations were large.



CURVE	INTERCEPTOR and POSITION	% INT.
1	.080" aperture —	0
2	.040" " at anode	45
3	" " at cavity	"
4	tilted grid at anode	50
5	" " at cavity	"

FIGURE 5-3 MAXIMA AND MINIMA OF NOISE IN THE DRIFT SPACE.



<u>CURVE</u>	<u>INTERCEPTOR</u> and <u>POSITION</u>	<u>% INT.</u>
1	.080" aperture —	0
2	.040" " at anode	45
3	" " at cavity	"
4	tilted grid at anode	50
5	" " at cavity	"

FIGURE 5-4 MAXIMA AND MINIMA OF NOISE IN THE DRIFT SPACE

The gross effects of interception on the space-charge wave can be explained on the basis of the theory outlined in Chapter 2, section III. At the intercepting electrode a new source of noise is created which establishes its own standing wave in the drift space. The total space-charge wave is the sum of the wave due to interception and the wave due to the noise in the beam before interception. The phase of the interception-noise wave is such that it always has a maximum at the intercepting electrode. As long as the plane of interception occurs at a maximum of the standing wave in the unintercepted beam, the resultant standing wave still exhibits deep minima. When the interception takes place at the cavity, the noise due to interception is a maximum and almost completely masks the space-charge wave due to initial noise.

Further confirmation of the theory was obtained as follows. The interception plate (tilted grid in the beam) was placed at a distance from the cavity equal to one quarter of a space-charge wavelength in the intercepted beam ( $\lambda_{q2}/4$ ). Thus, the cavity was measuring at a minimum of the standing wave. As the gun was withdrawn from its starting position at the interception plate, changes in the level of the minimum measured by the cavity were observed. These changes went through successive maxima and minima at anode-to-interception-plate distances which were correlated with the space-charge wavelength  $\lambda_{q1}$  in the unintercepted beam. The variation in noise level at the minimum is shown in Table 5-I as a function of the spacing between anode and interception plate. The noise level, denoted by  $\Gamma_C^2$ , has been normalized to shot noise.

TABLE 5-I

$\Gamma_C^2$  is the normalised noise level at the first minimum of the space-charge wave as a function of  $z$ , the spacing between anode and interception plate in units of  $\lambda_{q1}/4$

<u><math>\Gamma_C^2</math></u>	<u><math>z</math></u>
0.037	0
0.096	1
0.032	2
0.120	3
0.036	4
0.145	5

The interpretation of these measurements is shown in Figure 5-5. The wave B, due to interception noise, has a maximum at the point of interception and a minimum at the cavity. The wave A, due to original noise in the beam, has a minimum at the cavity if the spacing between gun anode and interception plate is

$$z = 2n \frac{\lambda_{q1}}{4}$$

Where  $\lambda_{q1}$  is the space-charge wavelength in the unintercepted beam, and  $n = 0,1,2,3,\dots$ . Similarly, wave A will have a minimum at the cavity for a spacing

$$z = (2n + 1) \frac{\lambda_{q1}}{4}$$

The cavity measures the noise power at the first minimum of wave C which is the sum of A and B.

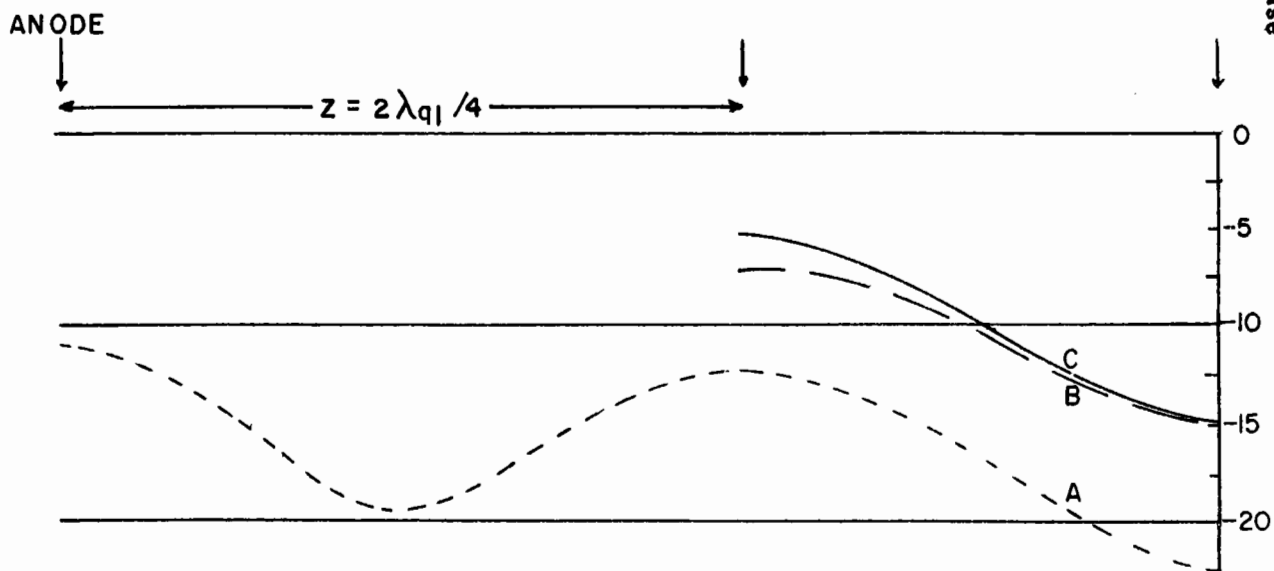
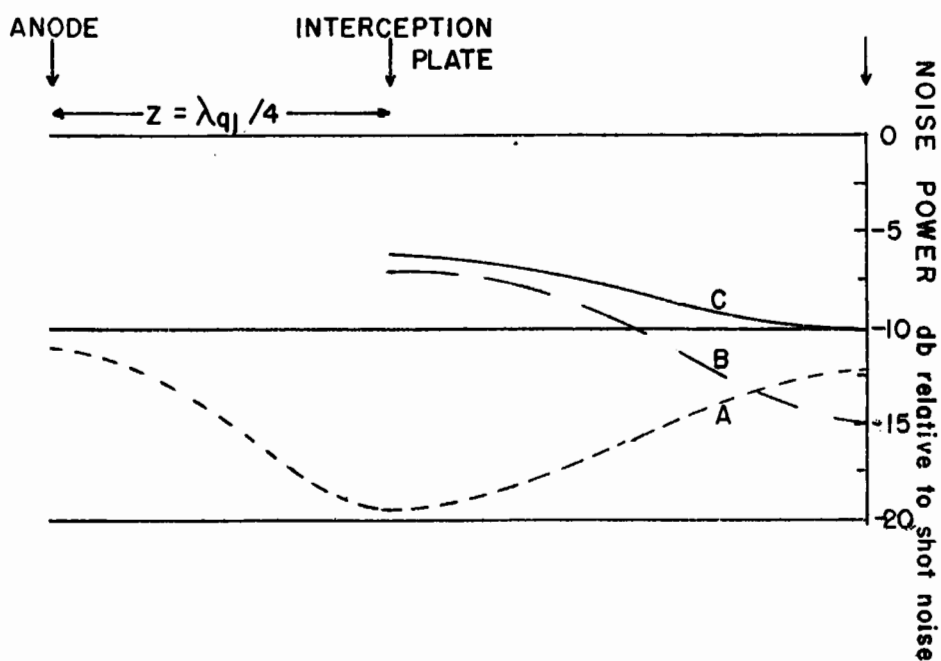
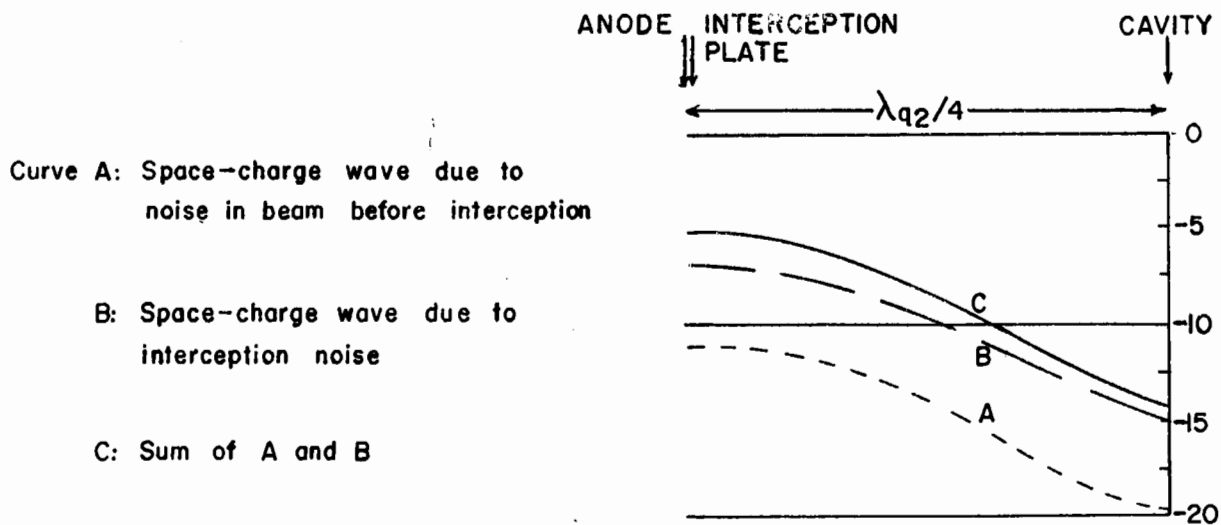


FIG. 5-5 ADDITION OF NOISE SPACE-CHARGE WAVES IN THE DRIFT SPACE

To be able to infer noise wave B (due to interception noise alone) from measurements made of wave C, it is necessary that wave A be known in the region between interception plate and cavity. It is argued in Appendix 3 that the only effect interception by a mesh grid has on a wave A is to increase the space-charge wavelength, provided that the noise power is normalized to shot noise before and after interception.

The values of  $\Gamma_A^2$  for the maxima and minima of wave A in the unintercepted beam may be obtained from Figure 5-3 (gun voltage 700 volts, curve 1). In Table 5-II these values are subtracted from the corresponding values of  $\Gamma_C^2$  listed in Table 5-I. The expected result is the value of  $\Gamma_B^2$  at the first minimum.

TABLE 5-II

$\frac{4z}{\lambda_{q1}}$	$\Gamma_C^2$	$\Gamma_A^2$	$\Gamma_B^2 = \Gamma_C^2 - \Gamma_A^2$
0	0.037	0.012	0.025
1	0.096	0.060	0.036
2	0.032	0.005	0.027
3	0.120	0.070	0.050
4	0.036	0.006	0.030
5	0.145	0.10	0.045

The error in values of  $\Gamma_C^2$  and  $\Gamma_A^2$  due to measurement and the normalization process is estimated as 0.4 db or 10%. Hence there is large possible error in values of  $\Gamma_B^2$ , in the table above, which arise from subtraction of nearly equal maxima. Since these are not true probable errors, it does not seem justified to weight the measurements inversely as the square of the

error. In order to obtain an average which does take into account possible error, the author has weighted the measurements as

$$\frac{1}{\text{possible error}}$$

The weighted average is then

$$\Gamma_B^2 \text{ average} = 0.031$$

with a standard deviation of  $\pm 0.007$ .

From this analysis it may be concluded that the space-charge wave due to interception noise alone has a phase angle, relative to the space-charge wave due to original noise, which depends on the distance between the anode plane and the plane of interception. This fact is of some importance in the design of beam-type microwave tubes. Minimization of the noise figure of a travelling-wave tube for example, requires a knowledge of the phase of the noise standing wave. It is apparent that interception of small amounts of current by the anode aperture will cause little increase in the noise figure.

In the case of the mesh grid, the ratio of maximum to minimum power in the space-charge wave due to interception noise alone is of the order of 10 db. It is interesting to compare this value with that predicted theoretically. Interception by a mesh grid provides a particularly useful case for two reasons. The noise level at the minima is sufficiently high that perturbing effects of secondary electrons may be discounted. The initial conditions for the wave are well defined; with a mesh grid, noise current and noise velocity are excited uniformly over the beam cross section. Hence the amplitudes of the higher order modes of the space-charge wave propagating in the beam may be calculated with some certainty. This is not the case for excitation of space-charge waves by noise at the anode of the

electron gun.

It is shown in Appendix 3 that interception-produced velocity noise and the higher order modes in the current noise wave contribute to a theoretical standing-wave ratio which is two orders of magnitude greater than that observed experimentally. On the basis of this analysis it seems likely that the observed low standing-wave ratio is due to d-c perturbations in the electron stream, ie. the radial variation of direct current density and possibly also scalloping which produces longitudinal variations in current density and in beam diameter.

(ii) Interception Noise on a Temperature-Limited Beam

Measurements of the variation of noise power with collector current, such as those illustrated by Figure 4-I, showed that, for a given value of collector current in the temperature-limited region, the noise power measured at the anode was not increased by interception. That is, the noise at the anode is full shot noise. Beyond the anode there are minima of the space-charge wave where the noise is less than full shot noise.

The noise level at the first standing-wave minimum in a temperature-limited beam was measured for various conditions of interception. A constant collector current of 50 microamperes was used. The cathode current was larger than this depending on the particular intercepting electrode used. Results are listed in Table 5-III.

TABLE 5-III

Interception noise on a temperature-limited beam.  $\Gamma_2^2$  is the noise level of the first standing-wave minimum in decibels below shot noise. Gun voltage = 700 volts; collector current = 50  $\mu$  a; magnetic field = 700 gauss.

<u>Interceptor</u>	<u>% Interception</u>	$\Gamma_2^2$ experimental	
		<u>Interceptor at anode</u>	<u>Interceptor at cavity</u>
.080" aperture	zero	12.7	12.7
.060" "	15 <sup>*</sup>	13.0	7.9 <sup>*</sup>
.040 "	57	14.0	5.0
tilted grid	45	11.5	3.0
flat grid	20	12.2	5.5

Note: <sup>\*</sup>These values are approximate averages which take into account large fluctuations in intercepted current due to scalloping on the beam.

These measurements provide conclusive evidence that interception noise can arise from a smoothing process external to the electron gun. The reduction of noise at the minima of the space-charge wave results from interactions which are completely independent of processes in the electron gun. Interception of current at a standing-wave minimum in a temperature-limited beam increased the noise in the same way qualitatively as it did at the anode of the gun when the emission was space-charge limited. Quantitatively, a comparison of the experimental values of  $\Gamma_2^2$  in Table 5-III with the corresponding values from Figure 5-2 for the space-charge limited case shows discrepancies that cannot be attributed to experimental error. Comparison of the two cases is made in Table 5-IV. Values of  $\Gamma_2^2$  predicted by the theories of North and of Beam are also tabulated.

The experimental results in column A are in closer agreement with values calculated according to Beam's theory. In contrast, with the exception of the .040" aperture, North's theory gives better agreement with the experimental results B for the temperature-limited case.

TABLE 5-IV

Comparison of noise smoothing in space-charge limited current with noise smoothing in temperature-limited current. Columns A are for space-charge-limited emission, smoothing measured at the anode (cf. Fig. 5-2, 700 volts). Columns B are for temperature-limited emission where smoothing was measured at the first minimum of the space-charge wave (cf. Table 4-I). The listed values of percent interception are only approximate since the exact values differed because of beam spreading.

		$\Gamma_2^2$ in decibels below shot noise					
		Experiment		Theory			
				North		Beam	
<u>Interceptor</u>	<u>% Interception</u>	A	B	A	B	A	B
.080" Aperture	Zero	11.2	12.7	-	-	-	-
.060" "	15	11.2	7.9	9.1	7.1	10.1	11.5
.040" "	50	10.8	5.0	2.2	2.4	9.6	10.8
Tilted grid	50	5.4	3.0	2.6	3.4	7.3	7.7
Flat grid	20	7.2	5.5	5.6	5.8	7.9	8.5

Before it is concluded that the magnitude of interception noise depends to some extent on the mechanism of smoothing, some effects of d-c perturbations should be considered. The Pierce type electron gun employs anode and cathode electrodes which are shaped so as to produce, at the edge of a space-charge-limited electron beam, an electrostatic field which matches the field due to space charge just inside the beam. That is, the finite beam behaves as a section taken from an infinite beam without disturbing the boundary conditions at the edge. When the cathode emission is temperature-limited and

the current density low, the potential configuration inside the beam is determined by the beam-forming electrodes and not by space charge. Radley (1958) has calculated this potential configuration in the beam, and it is apparent from his plot that a large radial component of electric field exists. This field will produce excess transverse velocity and consequently greater spiralling of the electrons in the confining magnetic field. Thus the mean spreading radius which determines the magnitude of interception noise will be greatly increased. The experimental values of  $\Gamma_2^2$  for the two grids are within 0.4 db of the North-theory value, which is indicative of the fact that the mean spreading radius was much larger than the effective radius of one grid module.

That greater spiralling of electrons, and consequent increase in effective beam diameter, did exist was also evident from measurements of the fraction of current intercepted by a circular aperture as the cathode temperature was varied. In the case of the .040" aperture, at low cathode temperatures the interception was 65%; as the cathode temperature was increased to space-charge limitation, the fractional interception dropped to 45%. McFarlane (1958a) has observed a more extreme defocussing action in electron guns when no confining magnetic field was used.

Although the magnitude of the effect of this d-c beam perturbation cannot be assessed quantitatively, it is felt to be sufficiently large to account for the higher interception noise observed in a temperature-limited beam.

## CHAPTER 6

### Conclusions

Measurements were made at a frequency 3000 mc/s of the noise smoothing at the anode of a parallel-flow Pierce-type electron gun. Interception of a fraction of the electron current by a circular aperture caused little increase in noise when the electron beam was confined by a strong magnetic field of 700 gauss. Fifty percent interception produced a decrease of only 0.5 db in approximately 10 db of smoothing. A mesh grid caused decreases in smoothing as great as 7 db for an equivalent fraction of current intercepted.

It has been shown in this thesis that a theory of interception noise, due to Beam (1955), based on the random probability of interception of electrons, is consistent with experimental results. The interception noise produced by various geometrical shapes of electrodes can be calculated on the basis of the concept of "mean spreading radius". This is essentially the radial distance, about any point on a cross section of the electron stream, over which the probability of random interception is uniform; it is determined by the distribution of random transverse velocities of the electrons. If the radius of an intercepting aperture is much larger than the mean spreading radius, the excess noise produced is small. If current is intercepted by a fine mesh grid, of a size such that the radius of one small opening in the grid is less than the mean spreading radius, the interception noise is large and approaches a constant value which is identical to that predicted by North's low-frequency theory.

When an electron beam is confined by a magnetic field, the mean spreading radius is inversely proportional to the strength of the magnetic field.

Measured values of interception noise decreased as the magnetic field was increased from 150 gauss to 700 gauss. Agreement between experimental values of smoothing and values predicted by Beam's theory was  $\pm 1$  db for a grid intercepting 20% of the electron beam current and for an aperture intercepting 50% of the current. For apertures intercepting current near the beam edge, slightly better agreement with experiment has been obtained by modifying Beam's theory to take into account the radial variation of direct current density in the electron beam. The actual variation of direct current density with radius was found to deviate widely from the theoretical form, and is believed to account for the fact that the measured excess noise, due to interception near the beam edge, was less than that predicted by theory.

The propagation of noise waves along a constant-velocity electron beam was studied, first with cathode emission limited by space charge in the electron gun. It was observed that interception of current excited a standing wave of noise along the beam that had a maximum of power at the plane of interception. The noise standing wave due to interception was independent of the wave due to noise of thermal origin. The two waves of noise power added with a phase relation determined by the spacing between gun anode and the plane of interception. In the noise standing wave produced by grid interception, finite minima were observed which were two orders of magnitude higher than could be explained theoretically. This was attributed to the radial variation of direct current density.

The theory of interception noise based on random interception of electrons requires no assumptions concerning the mechanism of smoothing as did North's theory. That interception noise can arise from a smoothing

process external to the electron gun has been demonstrated by the measurements of interception noise in a temperature-limited beam. Interception at the anode of the electron gun caused no excess noise, implying that the beam emerging from the gun was not smoothed. Interception at a minimum of the space-charge wave did create excess noise. The observed values of interception noise at the minimum of the standing wave were much higher than predicted by theory. This has been attributed to an increase in the mean spreading radius due to excess transverse velocity resulting from the distorted electrostatic field in the electron gun.

APPENDIX 1

I Evaluation of the  $\Omega_1$  and  $\Omega_2$  Integrals.

Since Beam's published curves do not provide sufficiently precise values of  $\Omega_1$  and  $\Omega_2$  for any choice of the variables  $a$ ,  $r_a$ ,  $r_b$ , analytic expressions were derived.

Equation (2-21) may be rewritten in the form

$$\Omega_1 = \int_0^1 [1 + \operatorname{erf} b(x - u)] u du \quad (\text{A-1})$$

where  $b = a r_b$ ,  $x = r_a/r_b$ .

Integration by parts yields

$$\begin{aligned} \Omega_1 = & \frac{1}{2} + \left[ \frac{x^2}{2} + \frac{1}{4b^2} \right] \operatorname{erf} bx \\ & - \left[ \frac{x^2}{2} + \frac{1}{4b^2} - \frac{1}{2} \right] \operatorname{erf} b(x - 1) \\ & + \frac{x}{2b\sqrt{\pi}} \exp(-b^2 x^2) - \frac{x+1}{2b\sqrt{\pi}} \exp[-b^2(x-1)^2] \quad (\text{A-2}) \end{aligned}$$

When  $x$  is less than unity,  $\operatorname{erf} b(x - 1)$  is negative. By rearranging,

$$\begin{aligned} \Omega_1 = & \left[ \frac{x^2}{2} + \frac{1}{4b^2} \right] \left[ \operatorname{erf} bx + \operatorname{erf} b(1 - x) \right] + \frac{1}{2} \left[ 1 - \operatorname{erf} b(1 - x) \right] \\ & + \frac{x}{2b\sqrt{\pi}} \exp(-b^2 x^2) - \frac{x+1}{2b\sqrt{\pi}} \exp[-b^2(1 - x)^2] \quad (\text{A-3}) \end{aligned}$$

The error function has value which differs from unity by less than 0.005 for argument greater than 2.0. In most cases of interest  $b > 10$ ; hence for  $x < 0.8$ , the only significant term in Equation (A-3) is the first.

$$\begin{aligned} \Omega_1 & \approx 2 \left[ \frac{x^2}{2} + \frac{1}{4b^2} \right] \\ & \approx x^2 = r_a^2/r_b^2 \quad (\text{A-4}) \end{aligned}$$

As  $x$  approaches unity,  $\Omega_1$  is still equal to  $r_a^2 / r_b^2$  with small error but the fractional interception  $1 - \Omega$ , must be calculated more precisely. For example, at  $r_a = r_b$ ,

$$\Omega_1 = 1 + \frac{1}{4b^2} - \frac{1}{b\sqrt{\pi}},$$

or

$$1 - \Omega_1 \approx \frac{1}{b\sqrt{\pi}} \quad (A-5)$$

The integral in Equation (2-22) for the  $\Omega_2$  function cannot be calculated exactly. However, the integrand may be approximated by the function

$$\exp \left[ -\frac{4}{\pi} b^2 (x - u)^2 \right] \quad (A-6)$$

with an error which is less than 0.01 for all significant values of the function. The integration may then be performed to yield,

$$\begin{aligned} \Omega_2 = & \frac{\pi}{8} \frac{x}{b} \left[ \operatorname{erf} \frac{2}{\sqrt{\pi}} bx + \operatorname{erf} \frac{2}{\sqrt{\pi}} b(1-x) \right] \\ & - \frac{\pi}{16b^2} \left\{ \exp \left[ -\frac{4}{\pi} b^2 (1-x)^2 \right] - \exp \left[ -\frac{4}{\pi} b^2 x^2 \right] \right\} \quad (A-7) \end{aligned}$$

For  $b > 10$  the error in neglecting the second bracket is never greater than 5% for all significant cases. Also, in most cases  $\frac{2}{\pi} bx > 2$  so that  $\Omega_2$  becomes

$$\Omega_2 = \frac{\pi}{8} \frac{r_a}{ar_b^2} \left[ 1 + \operatorname{erf} \frac{2}{\sqrt{\pi}} ar_a \left( \frac{r_b}{r_a} - 1 \right) \right] \quad (A-8)$$

It is easily shown that if  $r_a > r_b$ ,  $\Omega_2 \rightarrow 1 - \Omega_1$ . It may be recalled that

$$\Omega_2 = \frac{1}{2} \int_0^1 [1 + \operatorname{erf} b(x-u)] [1 - \operatorname{erf} b(x-u)] u du$$

If  $b(x-1) > 2$ , then  $1 + \operatorname{erf} b(x-u) = 2$  over the whole range of integration.

Thus,

$$\begin{aligned}\Omega_2 &\approx \int_0^1 [1 - \operatorname{erf} b(x - u)] \, u \, du \\ &\approx 1 - \int_0^1 [1 + \operatorname{erf} b(x - u)] \, u \, du \\ &\approx 1 - \Omega_1\end{aligned}$$

## II Numerical Calculations from Theory

It is necessary to calculate  $\Gamma_2^2$  from the equations

$$\Gamma_2^2 = \Gamma_1^2 + (1 - \Gamma_1^2) \frac{\Omega_2}{\Omega_1}$$

and

$$\frac{\Omega_2}{\Omega_1} = \frac{\pi}{8} \frac{1}{a r_a} \left[ 1 + \operatorname{erf} \frac{2}{\sqrt{\pi}} a r_a \left( \frac{r_b}{r_a} - 1 \right) \right]$$

The temperature of the oxide cathode for space-charge-limited emission was taken as 1350°k (Desrocher 1958). Thus the constant  $a$  is

$$a = 86.7 B \text{ (meters}^{-1}\text{)}$$

where B is the magnetic field strength in gauss.

The aperture radius  $r_a$  is a well defined value, but the beam radius  $r_b$  was difficult to determine since the beam diameter varied with magnetic field strength. However, except very near the beam edge, the fraction of current transmitted is equal to  $r_a^2/r_b^2$ , from which an effective value of  $r_b$  can be determined. Then the calculated values of  $\Omega_2/\Omega_1$  along with the experimental value of  $\Gamma_1^2$  (zero-interception smoothing) were used to calculate  $\Gamma_2^2$ .

For small amount of interception near the beam edge, the effective beam diameter is again determined by the measured value of the transmission factor  $\Omega_1$ , but not in so simple a manner as above. In these cases, the value of

$\Omega_2$  for a particular value of  $\Omega_1$  was read directly from the curves of  $\Omega_2$  versus  $1 - \Omega_1$  shown in Fig. A - 1. Here  $\Omega_2$  has been modified for the non-uniform current-density distribution of Equation (2-25).

In the case of the grids, an effective radius for each of the small beams associated with one grid opening may also be calculated from measured values of current interception. The effective radius of the hexagonal holes in the flat grid is

$$r_a = 1.78 \times 10^{-4} \text{ meters}$$

When a grid is tilted, the open areas looking in the direction of electron flow have the shape of flattened hexagons. An effective radius was taken as that of a circle having equal area. Since the angle of tilt was not known sufficiently accurately to permit a geometrical calculation, the effective area was calculated from experimental values of transmitted current.

Let each of the small holes in the flat grid have open area  $A_f$ . Then

$$\text{fraction of current transmitted} = \frac{N_f A_f}{A_{\text{beam}}} = 0.78$$

where  $N_f$  is the number of holes in the beam area  $A_{\text{beam}}$ . For the tilted grid,

$$\frac{N_t A_t}{A_{\text{beam}}} = 0.52$$

The angle of tilt was known sufficiently accurately to calculate the increase in the number of holes. That is

$$\frac{N_t}{N_f} = 1.06$$

Therefore,

$$\frac{A_t}{A_f} = 0.62$$

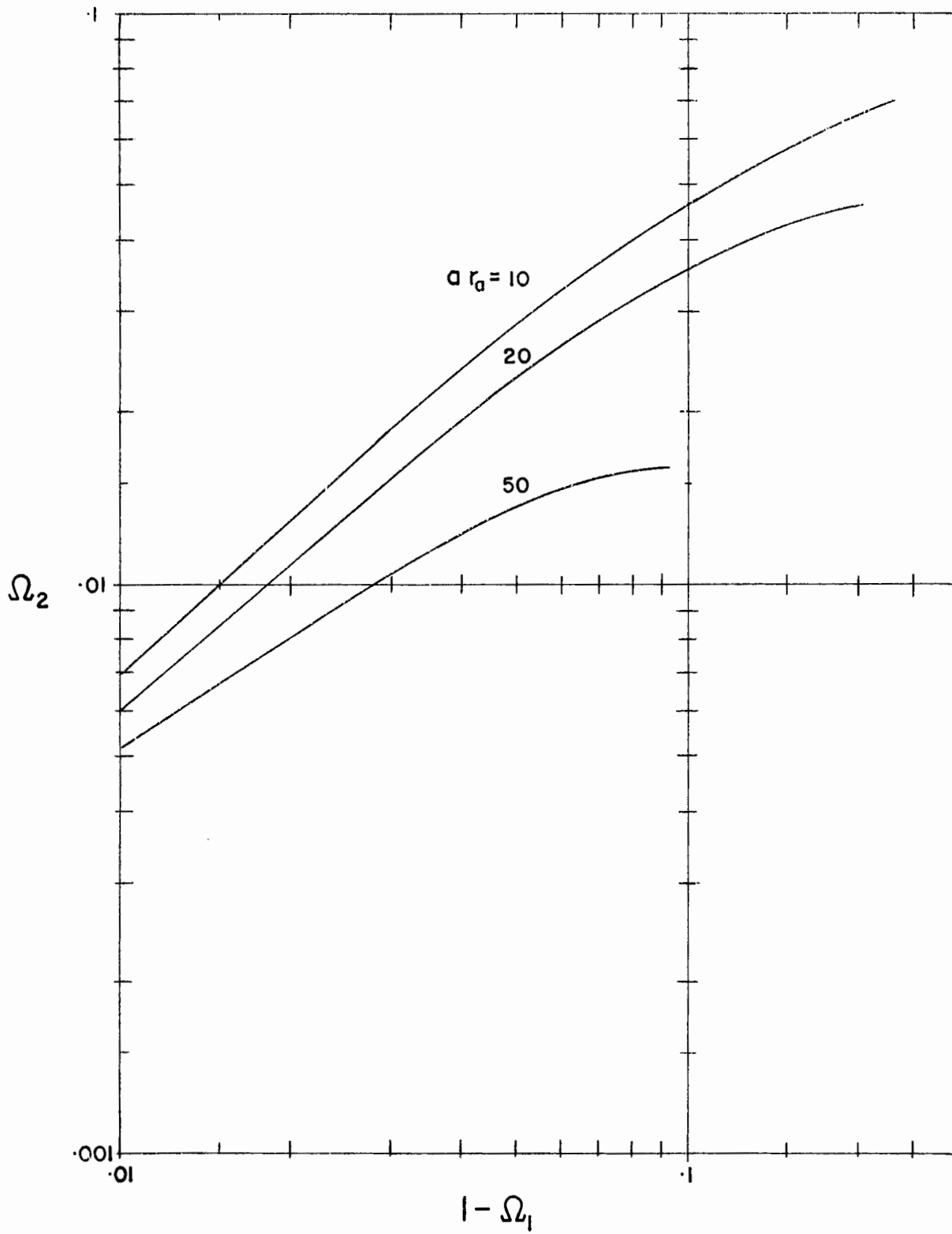


FIGURE A-1

And hence the ratio of effective radii is

$$\frac{r_{at}}{r_{af}} = 0.79$$

Finally,

$$r_a = 1.4 \times 10^{-4} \text{ meters for tilted grid.}$$

APPENDIX 2

The Problem of Non-Unity Slope

As has been mentioned in Chapter 4, noise power was observed to be proportional to  $I_0^n$  ( $n \leq 1$ ) for temperature-limited emission. Various solutions of the Electronic equation (Hutter 1952, 1953) have been examined in order to determine whether non-unity slopes could be attributed to an intrinsic variation of noise power not directly proportional to d-c beam current. The particular solution which results when the potential configuration in the electron gun region is determined by space charge leads to the Llewellyn-Peterson (1944) equations. In the true infinite beam case, for small space charge (temperature-limited emission) the potential variation is linear with distance coordinate  $z$ . In actual fact, in the Pierce type gun, the potential configuration for small space charge is determined by the shaped electrodes and varies at  $z^{4/3}$ . The electronic equation must then be solved for this potential variation.

Radley (1958) has shown the potential in the beam is a function of radius as well as longitudinal distance  $z$ ; but for simplicity, this will be ignored. It should also be noted that near the cathode the electron velocity is not single valued as assumed by the electronic equation.

Since the potential variation imposed by the shaped electrodes is identical to that in a beam with full space-charge, the d-c velocity  $u_0$  as a function of transit time  $\tau$  is: (Llewellyn 1941),

$$u_0 = \frac{1}{2} \frac{e}{m\epsilon_0} J'_0 \tau^2 + u_a \quad (A-9)$$

where  $J'_0$  is the d-c current density for full space-charge limited emission and  $u_a$  is the initial velocity at the cathode.  $u_a$  is taken equal

to the r.m.s. thermal velocity  $\sqrt{\frac{2kT_c}{m}}$ .

For a finite electron beam, the Electronic Equation as derived by Parzen (1952) is

$$\frac{d^2 Y}{d\tau^2} - \frac{1}{u_0} \left[ \frac{d^2 u_0}{d\tau^2} - \frac{ep^2 J_0}{m\epsilon_0} \right] Y = 0 \quad (A-10)$$

where:  $Y = J u_0 \exp(+j\omega\tau)$ ,  $J$  being the amplitude of the a-c current modulation;

$J_0$  is the actual direct-current density;  $p$  is the plasma reduction factor.

Let

$$k' = \frac{e}{m} \frac{J_0'}{\epsilon_0} .$$

Then

$$\frac{d^2 Y}{d\tau^2} - \frac{k'}{u_0} \left[ 1 - \frac{J_0}{J_0'} p^2 \right] Y = 0$$

For values of  $J_0$  in the temperature-limited region,  $\frac{J_0}{J_0'} \sim 10^{-3}$ , and since  $p^2$  has maximum value unity, the term  $\frac{J_0}{J_0'} p^2$  is negligible over the whole range of  $\tau$ . Thus (A - 10) may be written,

$$u_0 \frac{d^2 Y}{d\tau^2} - \frac{d^2 u_0}{d\tau^2} Y = 0 \quad (A - 11)$$

A first integration gives,

$$u_0 \frac{dY}{d\tau} - \frac{du_0}{d\tau} Y = C_1 \text{ a constant} \quad (A - 12)$$

The equation for the a-c velocity is,

$$v = \frac{1}{j\omega J_0 u_0} \left( u_0 \frac{dY}{d\tau} - \frac{du_0}{d\tau} Y \right) e^{-j\omega\tau}$$

Hence,

$$v = \frac{C_1}{j\omega J_0 u_0} e^{-j\omega\tau}$$

At the cathode we have the initial conditions  $\tau = 0, v = v_a, u_o = u_a$

Therefore

$$C_1 = j\omega J_o u_a v_a, \quad (\text{A-13})$$

or

$$v = \frac{u_a}{u_o} v_a e^{-j\omega\tau} \quad (\text{A-14})$$

Thus the gun region acts as a simple "velocity jump" as far as a-c velocity is concerned. (Hutter 1953; Watkins 1953)

Equation (A-12) may be written

$$\begin{aligned} u_o^2 \frac{d(Y/u_o)}{d\tau} &= C_1 \\ \frac{Y}{u_o} &= C_1 \int \frac{d\tau}{u_o^2} = C_1 \int \frac{d\tau}{(\frac{k}{2}\tau^2 + u_a)^2} \\ &= \frac{C_1}{k u_a} \left[ \frac{\tau}{\tau^2 + \delta} + \frac{1}{\sqrt{\delta}} \tan^{-1} \frac{\tau}{\sqrt{\delta}} \right] + C_2 \quad (\text{A-15}) \end{aligned}$$

$$\text{where } \delta = \frac{2u_a}{k}$$

Now,

$$J = \frac{Y}{u_o} e^{-j\omega\tau}$$

$$J = C_2 + \frac{j\omega J_o v_a}{k} \left[ \frac{\tau}{\tau^2 + \delta} + \frac{1}{\sqrt{\delta}} \tan^{-1} \frac{\tau}{\sqrt{\delta}} \right] e^{-j\omega\tau}$$

At the cathode  $\tau = 0, J = J_a$ . Therefore

$$J = J_a e^{-j\omega\tau} + \frac{j\omega J_o}{k} \left[ \frac{\tau}{\tau^2 + \delta} + \frac{1}{\sqrt{\delta}} \tan^{-1} \frac{\tau}{\sqrt{\delta}} \right] v_a e^{-j\omega\tau} \quad (\text{A-16})$$

The input conditions at the cathode are assumed to be full shot noise and the Rack velocity fluctuation. (Rack 1938).

That is

$$\overline{i_a^2} = 2e I_o \Delta f$$

$$\overline{v_a^2} = (4 - \pi) \frac{e}{m} \frac{kT_c}{I_o} \Delta f$$

Multiplying Equation (A-16) by the beam area yields the current fluctuation. Then the noise power is proportional to,

$$\overline{i_n^2} = \overline{i_a^2} + \left| \frac{j\omega I_0}{k} \left[ \frac{\tau}{\tau^2 + \delta} + \frac{1}{\sqrt{\delta}} \tan^{-1} \frac{\tau}{\sqrt{\delta}} \right] \right|^2 \overline{v_a^2}$$

At the anode  $\frac{\tau}{\sqrt{\delta}} \gg 1$ , so that  $\tan^{-1} \frac{\tau}{\sqrt{\delta}} = \frac{\pi}{2}$

With some rearranging,

$$\overline{i_n^2} = 2e I_0 \Delta f + \frac{(\omega\tau)^2 I_0^2}{4} \left[ \frac{1}{u_0} + \frac{1}{\sqrt{u_0 u_a}} \frac{\pi}{2} \right]^2 0.86 \frac{e}{m} \frac{kT_c}{I_0} \Delta f$$

The second term in the brackets is larger than the first, so that approximately,

$$\overline{i_n^2} = 2e I_0 \Delta f + \frac{0.86 \pi^2}{32} \frac{(\omega\tau)^2 kT_c}{m u_a u_0} 2e I_0 \Delta f$$

Substituting  $kT_c = \frac{1}{2} m u_a^2$ ,

$$\frac{\overline{i_n^2}}{2e I_0 \Delta f} = 1 + \frac{0.86 \pi^2}{64} (\omega\tau)^2 \frac{u_a}{u_0} \quad (A-17)$$

Since there is no term in the right hand side of Equation (A-17) that varies with a-c current  $I_0$ , unity slope is predicted for the shot noise asymptote.

A cavity, measuring noise at the anode of the gun, responds also to the a-c velocity of Equation (A-14). However, it can be shown (Kornelsen 1957), that if the cavity gap is narrow, the power contributed by the a-c velocity is insignificant compared to the power due to the a-c current. This is true of the cavity used in these experiments.

The foregoing simplified theory neglects possible effects due to the multivelocity nature of the electrons flow near the cathode and to the higher order modes of propagation that exist in a finite beam. Further, the

radial component of the d-c electric field in the gun has been neglected. This is known from experimental measurements to cause considerable spreading of the electron beam for temperature-limited emission. That is, the beam radius is known to be large for small beam currents and to decrease as beam current increases towards space-charge limitation.

The power coupled from the beam to the cavity is proportional to a factor  $M^2$  which varies with beam radius  $r_b$ . This is given by (Warnecke and Guenard 1951),

$$M^2 \propto \frac{I_1(\theta_b)/\frac{\theta_b}{2}}{I_0(\theta_c)}$$

where

$$\theta_b = \frac{\omega r_b}{u_0}, \quad \theta_c = \frac{\omega r_c}{u_0},$$

$r_c$  being the radius of the cavity hole.  $I_1$  and  $I_0$  are modified Bessel functions. For a change in beam radius, the fractional variation in  $M^2$  is

$$\frac{dM^2}{M^2} = 4 \frac{d\theta_b}{\theta_b} \left[ \frac{\theta_b^2}{8} + \frac{2}{3} \frac{\theta_b^4}{64} + \dots \right] \\ \frac{d r_b}{r_b} \frac{\theta_b^2}{2}, \quad (\text{A-18})$$

since  $\theta_b$  is of the order of unity or less. Thus the percent variation in power is of the same order as the percent variation in beam radius. This effect is larger for lower gun voltages ( $u_0$  smaller and hence  $\theta_b$  larger) which is in agreement with the observed variation of slope with gun voltage.

A detailed examination of the experimental evidence was at best inconclusive, and at worst, contrary to this hypothesis. In these experiments, the diameter of the beam transmitted through the cavity could be maintained constant by the use of the .040" aperture, but still non-unity slopes were

measured. There was no significant difference among the slopes measured for 3 different sized apertures. One could postulate a drastic change in the radial current density distribution with beam current, but this effect should be negligible for the .040" aperture.

Further, within the accuracy of measurement of interception current, the fractional interception was constant over the straight-line portion of the smoothing curve and began to decrease just at the point where the smoothing curve breaks from a straight line.

Another effect that was investigated was the change in beam diameter due to scalloping. If the length or position of the scallop waves were to change with beam current, it would change the effective beam diameter seen by the cavity. Measurements showed that the scallop wavelength was equal to the theoretical "cyclotron" wavelength over a wide range of current, and that shift in the position of the scallop pattern with current was negligible. As further evidence, slopes measured for different magnetic field strengths showed no significant variation.

APPENDIX 3

Some Space-Charge Wave Calculations

I Matching across a plane of interception

We wish to examine the effect of current interception on the noise space-charge wave that existed in the beam before interception. That is, we exclude the added noise due to interception.

In the unintercepted beam, the a-c current and velocity as a function of distance are

$$i_1(z_1) = i_a \cos \theta_1 - j \frac{\omega}{\omega_{q1}} \frac{I_{o1}}{u_0} v_a \sin \theta_1 \quad (A-19)$$

$$v_1(z_1) = v_a \cos \theta_1 - j \frac{\omega_{q1}}{\omega} \frac{u_0}{I_{o1}} i_a \sin \theta_1$$

where  $\theta_1 = \frac{\omega_{q1} z_1}{u_0}$ . The subscript 1 is used to denote quantities before interception.  $i_a$  and  $v_a$  are the initial excitations at a plane  $z_1 = 0$  and are assumed uncorrelated. Let

$$\overline{i_a^2} = \Gamma_a^2 2e I_{o1} \Delta f$$

Now,

$$\omega_{q1} = p \omega_{p1}$$

where

$$\omega_{p1}^2 = \frac{e}{\epsilon_0 m} \frac{I_{o1}}{u_0}$$

Thus we have

$$\begin{aligned} \frac{\overline{i_1^2}}{2e I_{o1} \Delta f} &= \frac{\omega^2}{2e^2 p^2 u_0 \Delta f} \frac{\overline{v_a^2}}{\epsilon_0 m} \sin^2 \theta_1 + \Gamma_a^2 \cos^2 \theta_1 \\ &= \frac{\Gamma_a^2 + K \overline{v_a^2}}{2} + \frac{\Gamma_a^2 - K \overline{v_a^2}}{2} \cos \frac{4\pi z_1}{\lambda_{q1}} \end{aligned} \quad (A-20)$$

$$\text{where } K = \frac{\omega^2 \epsilon_0 m}{2p^2 e^2 u_0 \Delta f}$$

Similarly,

$$K \frac{\bar{v}_1^2}{v_1} = \frac{\Gamma_a^2 + K \bar{v}_a^2}{2} - \frac{\Gamma_a^2 - K \bar{v}_a^2}{2} \cos \frac{4\pi z_1}{\lambda_{q1}} \quad (\text{A-21})$$

In the case of interception by a mesh grid, the beam diameter is unchanged. Therefore  $p$ , and hence  $K$ , are the same on both sides of the plane of interception. Suppose the plane of interception is located at  $z_1 = L$ .

It has been argued in Chapter 2 that,

$$\left. \frac{\bar{i}_1^2}{2e I_{o1} \Delta f} \right|_{L^-} = \left. \frac{\bar{i}_2^2}{2e I_{o2} \Delta f} \right|_{L^+}$$

Also

$$\left. \bar{v}_1^2 \right|_{L^-} = \left. \bar{v}_2^2 \right|_{L^+}$$

Write Equation (A-20) in the form

$$\frac{\bar{i}_1^2}{2e I_{o1} \Delta f} = A_1 + B_1 \cos \frac{4\pi z_1}{\lambda_{q1}}$$

After interception the plasma wavelength will be

$$\lambda_{q2} = \frac{2\pi u_0}{p \omega_p^2} = \frac{2\pi u_0}{p} \sqrt{\frac{\epsilon_0 m u_0}{e I_{o2}}}$$

The normalized current wave after interception will have the form,

$$\frac{\bar{i}_2^2}{2e I_{o2} \Delta f} = A_2 + B_2 \cos \left( \frac{4\pi z_2}{\lambda_{q2}} + \epsilon \right)$$

where  $z_2$  is measured from the plane of interception.

Matching the current and velocity at the plane of interception yields,

$$A_1 + B_1 \cos \frac{4\pi L}{\lambda_{q1}} = A_2 + B_2 \cos \epsilon$$

$$A_1 - B_1 \cos \frac{4\pi L}{\lambda_{q1}} = A_2 - B_2 \cos \epsilon$$

Therefore

$$A_2 = A_1, \quad B_2 \cos \epsilon = B_1 \cos \frac{4\pi L}{\lambda_1}$$

Suppose the measuring cavity is placed at  $z_2 = \frac{\lambda_{q2}}{4}$ . Then

$$\begin{aligned} \frac{\overline{i_2^2}}{2e I_{o2} \Delta f} &= A_2 - B_2 \cos \epsilon \\ &= A_1 - B_1 \cos \frac{4\pi L}{\lambda_{q1}} \end{aligned}$$

When  $L$  is varied as in the experiment described in Chapter 5, Section III, the variation in noise power will be the same as for the unintercepted beam.

## II The Space-Charge Wave due to Interception Noise alone.

(i) The contribution of added velocity fluctuations: We now consider the space-charge wave excited by the interception-produced current and velocity fluctuations which are given by

$$\begin{aligned} \overline{i_i^2} &= (1 - \Gamma_1^2) \frac{\Omega_2}{\Omega_1} 2e I_{o2} \Delta f \\ \overline{v_i^2} &= \left( \frac{kT_c}{mu_o} \right)^2 \frac{\Omega_2}{\Omega_1} \frac{2e}{I_{o2}} \Delta f \end{aligned}$$

We may neglect  $\Gamma_1^2$  compared with 1. The current space charge wave is,

$$\begin{aligned} \overline{i_2^2} &= \overline{i_i^2} \cos^2 \theta_2 + \left( \frac{\omega}{\omega_{q2}} \frac{I_{o2}}{u_o} \right)^2 \overline{v_i^2} \sin^2 \theta_2 \\ \frac{\overline{i_2^2}}{2e I_{o2} \Delta f} &= \frac{\Omega_2}{\Omega_1} \cos^2 \theta_2 + \left( \frac{\omega}{\omega_{q2}} \right)^2 \left( \frac{kT_c}{mu_o} \right)^2 \frac{\Omega_2}{\Omega_1} \sin^2 \theta_2 \end{aligned}$$

The ratio of maximum to minimum power is,

$$\text{Standing-Wave Ratio} = \frac{1}{\left( \frac{\omega}{\omega_{q2}} \right)^2 \left( \frac{kT_c}{mu_o} \right)^2}$$

For gun voltage = 700 volts and cathode temperature  $T_c = 2300^\circ\text{K}$ ,

$$\text{S.W.R} \sim 3 \times 10^4$$

(ii) Propagation of higher order modes: The foregoing theory deals essentially with the fundamental, or first order, mode of propagation in a finite electron beam. Since the higher order modes propagate with wavelengths different from that of the fundamental mode, they will contribute finite power at the minima of the noise standing wave where the amplitude of the fundamental mode goes to zero.

The noise current density is given by (Hahn 1939; Ramo 1939)

$$J(r, z) = \sum_n A_n J_0(T_n r) \cos(p_n \omega_p \frac{z}{u_0})$$

Where  $T_n$  is the radial propagation factor for the  $n$ 'th mode, and  $p_n$  is the plasma frequency reduction factor for the  $n$ 'th mode.

When the conducting wall surrounding the beam is infinitely remote (a distance equal to a few times the beam diameter is sufficient),  $T_n$  is the  $n$ 'th root of the equation specifying the boundary conditions:

$$T_n r_b \frac{J_1(T_n r_b)}{J_0(T_n r_b)} = \beta_e r_b \frac{K_1(\beta_e r_b)}{K_0(\beta_e r_b)}$$

$$\text{where } \beta = \frac{\omega}{u_0}$$

In the case of interception by a mesh grid, noise current density is excited uniformly over the beam cross section. Then at  $z = 0$ ,  $J(r, 0)$  is a constant  $\Lambda$  say, which may be expanded in terms of an orthogonal set of modes subject to the boundary condition specified above. Sneddon (1951) shows that the proper series is

$$J(r, z) = \frac{2}{r_b^2} \sum_n \frac{T_n^2 \bar{J}}{T_n^2 + G^2} \frac{J_0(T_n r)}{J_0(T_n r_b)} \cos(p_n \frac{\omega_p z}{u_0})$$

$$\text{where } G = \beta_e \frac{K_1(\beta_e r_b)}{K_0(\beta_e r_b)}$$

and  $\bar{J}$  is the finite Hankel transform

$$\bar{J} = \int_0^{r_b} \Lambda J_0(T_n r) r dr = \Lambda \frac{r_b}{T_n} J_1(T_n r_b)$$

If the current density is integrated across the beam, the current is given by

$$i(z) = \Lambda \pi r_b^2 \sum_n \frac{4(\frac{G r_b}{T_n r_b})^2}{(T_n r_b)^2 + (G r_b)^2} \cos p_n \frac{\omega_p z}{u_0}$$

The mode amplitudes are given in the following table.

Mode number "n"	$p_n$	$\frac{4(G r_b/T_n r_b)^2}{(T_n r_b)^2 + (G r_b)^2}$	amplitude at first minimum
1	0.547	0.980 <sub>1</sub>	0
2	0.217	0.021 <sub>9</sub>	0.0178
3	0.127	0.002 <sub>6</sub>	0.0024
4	0.089	0.000 <sub>7</sub>	-

Thus 98% of the current is excited in the first mode and the standing-wave ratio (power) at the first minimum is

$$S.W.R. \approx 2 \times 10^3$$

Consider the effect of radial variation of cavity coupling. The cavity coupling factor is proportional to

$$\frac{I_0(\beta_e r)}{I_0(\beta_e r_c)}$$

where  $r_c$  is the radius of the cavity aperture. When this factor is taken

into account, the amplitude of the n'th anode is given by

$$\frac{i_n}{\pi r_b^2 \Lambda} = \frac{2}{I_0(\beta_e r_c) K_1(\beta_e r_b)} \frac{\frac{T_n}{\beta_e} J_1(T_n r_b)}{(T_n r_b)^2 + (\beta_e r_b)^2}$$

The amplitude of the first mode is reduced to 0.686 while the amplitudes of higher modes are not changed significantly. This reduces the S.W.R. slightly, but it is still two orders of magnitude higher than that observed experimentally.

APPENDIX 4

The current density in an electron beam confined by a magnetic field may be calculated by a method similar to that used by Cutler and Hines (1955) to calculate thermal velocity spreading in converging electron guns.

As in Chapter II, attention is focussed on all those electrons which execute spirals about a given line in the electron beam. The intersection of this line with a plane perpendicular to the beam is indicated as P' in Figure A-2. In the absence of the magnetic field, the electrons associated with P' would have come from an equivalent point P<sup>0</sup> on the cathode. Because of the magnetic field they are spread over a much larger area and some will contribute to the current density at P. Thus the current density at P is a result of contributions from all points P' on the cathode surface.

The radial distribution of electrons about P' is given by (Equation 2-18)

$$\frac{dN_p}{N_{P'}} = 2a^2 \exp \left[ -a^2 \rho^2 \right] \rho d\rho$$

Or, in terms of cartesian coordinates centred at P',

$$\frac{dN_{x,y}}{N_{P'}} = \frac{a^2}{\pi} \exp \left[ -a^2 (x^2 + y^2) \right] dx dy$$

If J<sub>0</sub> is the current density at the cathode surface, the current associated with P' is

$$I_{P'} = J_0 dx' dy' = e N_{P'} dx' dy'$$

Then the current at P is

$$dI_P = J_0 dx' dy' \frac{a^2}{\pi} \exp \left[ -a^2 (x^2 + y^2) \right] dx dy$$

The current density at P is

$$dJ_P = \frac{dI_P}{dx dy} = J_0 \frac{a^2}{\pi} \exp \left[ -a^2 (x^2 + y^2) \right] dx' dy'$$

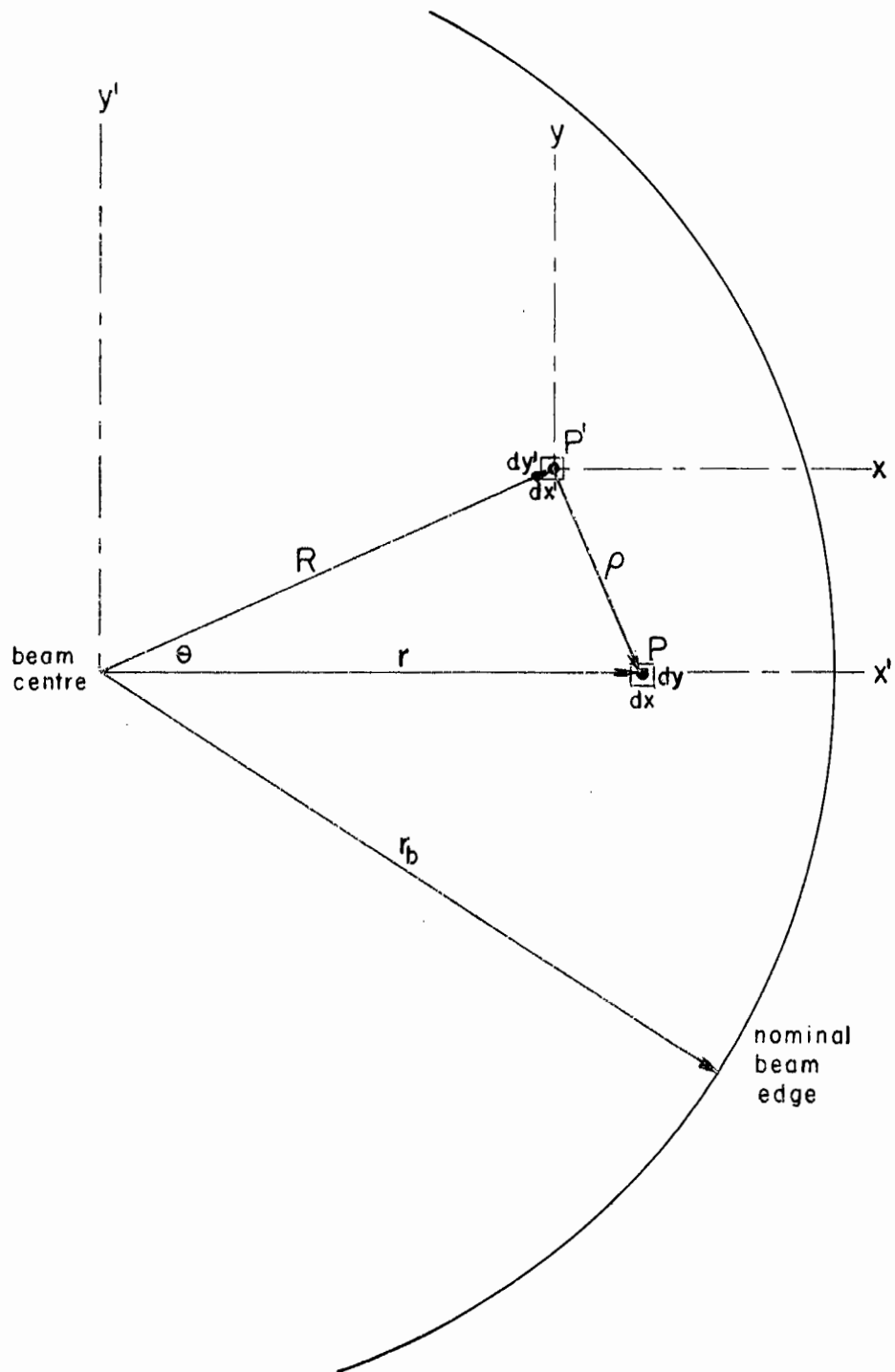


FIGURE A-2

This equation must be integrated over the total cathode surface. Referring to Fig. A-2, the limits of integration are  $R = 0$  to  $R = r_b$ ,  $\theta = 0$  to  $\theta = 2\pi$ . Cutler and Hines have carried out this integration numerically. In cartesian coordinates, the integration may be carried out if the following approximation is made. For strong magnetic fields,  $a$  is large and the distribution about  $P'$  is sharply peaked. The only significant contributions to the current at  $P$  are from points  $P'$  very close to  $P$ . The nominal beam edge, i.e. the cathode edge, may be approximated by a straight line perpendicular to  $r$ . The limits of integration in the cartesian system  $x'$ ,  $y'$  are then:  $y' = -\infty$  to  $y' = +\infty$ ,  $x' = -\infty$  to  $x' = r_b$ .

$$\begin{aligned}\text{Now, } x' &= r - x \\ y' &= y\end{aligned}$$

Therefore the integral becomes,

$$J_p(r) = J_0 \frac{a^2}{\pi} \int_{-\infty}^{+\infty} \int_{-\infty}^{r_b-r} \exp[-a^2(x^2 + y^2)] dx dy$$

or

$$\frac{J(r)}{J_0} = \frac{1}{2} \left[ 1 + \operatorname{erf} a(r_b - r) \right]$$

REFERENCES

- Ashkin, A. 1957, J. Appl. Phys. 28, 564.
- Beam, W. R. 1955, RCA Review 16, 551.
- Beck, A. H. W. 1957, Jour. of Electronics 2, 489.
- Cutler, C. C. and Quate, C. F. 1950, Phys. Rev. 80, 875.
- Cutler, C. C. and Hines, M.E. 1955, Proc. IRE 43, 307.
- Cutler, C. C. and Saloom, J. A. 1955, Proc. IRE 43, 299.
- Desrocher, L. G. 1958, M.Sc. Thesis, McGill University.
- Dicke, R. H. 1946, Rev. Sci. Inst. 17, 266.
- Fried, C. and Smullin, L. D. 1954, Trans. IRE, PGED-2, ED-1, 168.
- Fry, T. C. 1921, Phys. Rev. 17, 441.
- Goldman, S. 1948, Frequency Analysis, Modulation and Noise, McGraw-Hill.
- Hahn, W. C. 1939, Gen. Electric Review 42, 258.
- Hamilton, Knipp and Kuper 1948, Klystrons and Microwave Triodes, M. I. T. Rad. Lab. Series No.7, McGraw-Hill.
- Hauss, H. A. 1955, J. Appl. Phys. 26, 560.
- Hutter, R. G. E. 1952, Sylvania Technologist 5, 94;  
1953, Sylvania Technologist 6, 6.
- Kornelsen, E. V. 1957, Ph.D. Thesis, McGill University.
- Langmuir, I. 1923, Phys. Rev. 21, 419.
- Llewellyn, F. B. 1941, Electron Inertia Effects, Cambridge University Press.
- Llewellyn, F. B. and Peterson, L. C. 1944, Proc. IRE 32, 144.
- MacDonald, D. K. C. 1948a, Research 1, 194; 1948b, Rep. on Prog. Phys. 12, 56.
- McFarlane, R. A. 1956, Internal Eaton Electronics Research Laboratory Technical Report; 1958(a) Private communication.  
1958(b) Ph.D. Thesis, McGill University.
- North, D. O., et al, 1940a, RCA Review 4, 269;  
1940b, RCA Review 4, 441;  
1940c, RCA Review 5, 244.

- Parzen, P. 1952, J. Appl. Phys. 23, 215.
- Peterson, L. C. 1947, Proc. IRE 35, 1264.
- Pierce, J.R. 1949, Theory and Design of Electron Beams, D. Van Nostrand;  
1950, Travelling-Wave Tubes, D. Van Nostrand;  
1954, J. Appl. Phys. 25, 931.
- Rack, A. J. 1938, Bell Syst. Tech. J. 17, 592.
- Radley, D. E. 1958, Jour of Elect. and Control 4, 125.
- Ramo, S. 1939, Proc. IRE 27, 757.
- Rice, S. O. 1944, Bell Syst. Tech. J. 23, 282;  
1945, Bell Syst. Tech. J. 24, 46.
- Robinson, F. N. H. 1952, Phil. Mag. 43, 51;  
1954, J. Brit. IRE 14, 79.
- Robinson, F. N. H. and Kompfner, R. 1951, Proc. IRE 39, 918.
- Rowe, H. E. 1952, Sc. D. Thesis, M.I.T.
- Schottky, W. 1918, Ann. Physik 57, 541;  
1938, Ann. Physik 32, 195.
- Schottky, W. and Spenke, E. 1937, Wiss, Veroff. Siemens-Werken 16, 1.
- Shkarofsky, I. 1957, Ph.D. Thesis, McGill University.
- Smullin, L. D. 1951, J. Appl. Phys. 22, 1496.
- Watkins, D. A. 1952, Proc. IRE 40, 65;  
1953, Proc. IRE 41, 1741.
- Van der Ziel, A. 1954, Noise, Prentice-Hall.
- Vessot, R. F. C. 1957, Ph.D. Thesis, McGill University.
- Warnecke, R. and Guenard, P. 1951, Les Tubes Electroniques a Commande par Modulation de Vitesse; Gauthier-Villars, Paris.
- Yadavalli, S. V. 1955, J. Appl. Phys. 26, 605.